SCIENTIFIC COMMITTEE
EIGHTEENTH REGULAR SESSION

ELECTRONIC MEETING
10 – 18 August 2022

Final report on bomb radiocarbon age validation for yellowfin and bigeye tunas in the WCPO (Project 105) - 2022

WCPFC-SC18-2022/SA-IP-14a

Allen Andrews[1], Kei Okamoto[2], Keisuke Satoh[2], Caroline Welte[3,4], Paige Eveson[5], Francois Roupsard[6], Jed Macdonald[6], Bryan Lockheed[7], Jessica Farley[5]

[1] University of Hawaii, Manoa, Hawaii & Scientific Inquiries and Innovations – Age and Longevity Research Lab
[2] National Research and Development, Japan Fisheries Research and Education, Fisheries Resources Institute, Yokohama-shi, Japan
[3] Laboratory of Ion Beam Physics, ETHZ, Otto-Stern Weg 5 HPK, 8093 Zurich, Switzerland
[4] Geological Institute, ETH Zurich, Sonneggstrasse 5, 8092 Zürich, Switzerland
[5] CSIRO Environment, Hobart, Tasmania, Australia
[6] Pacific Community - SPC, Noumea, New Caledonia
[7] Department of Earth Sciences, Uppsala University, Uppsala, Sweden

Final report on bomb radiocarbon age validation for yellowfin and bigeye tuna in the WCPO (Project 105) – 2022

Allen Andrews[1], Kei Okamoto[2], Keisuke Satoh[2], Caroline Welte[3,4], Paige Eveson[5], Francois Roupsard[6], Jed Macdonald[6], Bryan Lockheed[7], Jessica Farley[5]

1. Executive summary

This paper describes the results for Project 105 aimed at using bomb radiocarbon (^{14}C) dating to test the accuracy of age estimates from purported annual growth zones in otolith sections of yellowfin (YFT) and bigeye (BET) tuna of the western and central Pacific Ocean (WCPO). A total of 134 otoliths from archived young-of-the-year (yoy) YFT, BET and skipjack (SKJ) specimens were analysed for ^{14}C with accelerator mass spectrometry (AMS), which were combined with 29 existing BET yoy ^{14}C measurements previously analysed in Japan, for a total of 163 measurements covering 30 years of otolith formation dates (1989 to 2019). The yoy tuna ^{14}C time series exhibited a strong concordance with the existing collective coral-otolith ^{14}C reference chronology for the tropical and subtropical Pacific Ocean. A series of 142 otoliths from older YFT aged 1 to 14 years and BET aged 1 to 13 years were sampled for the earliest growth (core extraction within the first year of growth) and analysed for ^{14}C led to successful measurements for 76 YFT and 64 BET. The post-peak ^{14}C decline exhibited by both the reference chronology — a combination of existing coral and otolith ^{14}C records with the yoy tuna ^{14}C chronologies from this study — and the calculated birth years derived from otolith growth zone counts for each species were in alignment with no significant differences in regression slopes and a minor potential age estimation bias of +0.5 year for YFT and no bias for BET. Hence, the use of thin otolith sections to age YFT and BET in the WCPO up to teenage lifespans is supported and the age reading protocol currently used is confirmed to be quantifying annual growth zone structure.

2. Introduction

As demonstrated in the recent assessments of WCPO BET (McKechnie et al., 2017; Vincent et al., 2018; Ducharme-Barth, et al. 2020), the specification of growth in integrated stock assessment models, such as MULTIFAN-CL, can have profound effects on stock status indicators. Hence, it is essential that such assessments use the best age data and growth model estimates available. To this end, WCPFC in recent years has commissioned extensive research efforts to collect and analyse BET (Farley et al., 2018; 2019; 2020b), and more recently YFT (Farley et al., 2020b), otoliths to estimate growth to inform stock assessments. This work has relied mostly on counting presumed annual opaque zones in otolith sections to provide the basis for determining age. Direct age validation of the otolith age reading was made through an analysis of several strontium chloride ($SrCl_2$) marked tuna otoliths that were tagged and recaptured. This validation is relatively limited, particularly for YFT, and a recent workshop held at IATTC on BET and YFT growth made the following conclusion (Farley et al., 2019): "Further direct age validation studies for bigeye and yellowfin daily and annual ageing methods, spanning the entire size range and expected range of longevity, are urgently needed in the Pacific."

[1] University of Hawaii, Manoa, Hawaii & Scientific Inquiries and Innovations – Age and Longevity Research Lab

[2] National Research and Development, Japan Fisheries Research and Education, Fisheries Resources Institute, Yokohama-shi, Japan

[3] Laboratory of Ion Beam Physics, ETHZ, Otto-Stern Weg 5 HPK, 8093 Zurich, Switzerland

[4] Geological Institute, ETH Zurich, Sonneggstrasse 5, 8092 Zürich, Switzerland

[5] CSIRO Environment, Hobart, Tasmania, Australia

[6] Pacific Community - SPC, Noumea, New Caledonia

[7] Department of Earth Sciences, Uppsala University, Uppsala, Sweden

Age reading protocols for tuna species have evolved toward the use of presumed annual growth zone counting, a method that typically generates ages that are greater than previous age reading protocols (e.g., Farley et al. 2006, Griffiths et al. 2010, Williams et al. 2013). For YFT and BET in the western North Atlantic - Gulf of Mexico, an otolith thin sectioning technique led to teenage lifespan estimates that were validated with bomb ^{14}C dating (Andrews et al., 2020). The innovative approach was to use the post-peak bomb ^{14}C decline period (~1980–2000) to corroborate YFT aged 2 to 18 years and BET aged 3 to 17. The findings provided a valid basis for determination of life history parameters that were quite different from previous age and growth assessments (Pacicco et al., 2021, Waterhouse et al., 2022), results that were similar to YFT and BET growth characteristics described for the WCPO (Farley et al. 2020b). This novel age validation methodology is well-suited to shorter lived tropical species and was recently applied successfully to Pacific bluefin tuna (*Thunnus orientalis*; Ishihara et al., 2017) and giant trevally in Hawaii (*Caranx ignobilis*; Andrews 2020). The approach compares otolith ^{14}C levels in the core (earliest growth) with a ^{14}C reference time-series for the region of interest, often a date-validated coral core chronology (e.g., Kalish, 1993; Campana 1999), to determine if the calculated birth year from otolith growth zone counts is consistent with the ^{14}C reference (e.g., Andrews et al., 2012; 2013). In general, an age reading protocol is considered valid if the collective birth years from across all age classes provides no bias relative to the ^{14}C reference chronology (i.e., an offset of the measured otolith ^{14}C values in time). While measured ^{14}C levels from an individual fish typically cannot provide a specific validated age due to uncertainty within the post-peak ^{14}C reference, it is the combined and replicated age reading across all age classes and their overall alignment that can be used to corroborate the protocol used to estimate age, as well as eliminate other possible growth scenarios that provide significantly different maximum age estimates, like estimated ages from overcounting in the earliest otolith growth structure (e.g., Andrews and Scofield 2021).

3. Objectives

The project purpose is to evaluate age estimates from otolith thin-section age reading for YFT and BET from the WCPO using bomb ^{14}C dating.

The project will:

- Establish a reference time series for bomb-produced ^{14}C as a baseline for older aged fish using the otoliths of yoy YFT and BET collected through time from the WCPO.
- Test the validity of adult YFT and BET age and longevity estimates derived from otolith growth zone counts, as well as the age reading protocol, with the new regional ^{14}C reference chronology.
- Investigate the uptake of ^{14}C within individual YFT and BET otoliths through ontogeny using the rostrum tip of large adults in comparison with the otolith core (a substitution for LA-AMS due to specimen and instrument limitations).

4. Results and discussion

Bomb-produced ^{14}C reference chronology

Prior to selection of yoy tuna otoliths for use as part of the post-peak ^{14}C reference series, data on existing coral and known date-of-formation otolith (young fish used as reference material) records from the subtropical and tropical Pacific Ocean were assembled. This collective record is built on an analysis of temporal constraints for mixed layer ^{14}C levels across this broad region in a study of a grander (≥1000 lb; 1 lb = 0.45 kg) blue marlin (*Makaira nigricans*) that was aged to 20 years using the temporal constraints of this composite reference chronology (see Andrews et al. (2018) for details on the ^{14}C reference composition). Since the time of the blue marlin research, additional ^{14}C records have become available from both coral cores and otoliths of juvenile fish, which were added to the

reference chronology used in this study. Included in this series are: 1) recent coral and otolith ^{14}C references from American Samoa that extend to 2015, including an analysis of dissolved inorganic ^{14}C across the South Pacific Gyre (Andrews et al., 2021b), and 2) a coral core from the Great Barrier Reef that covers the bomb ^{14}C signal through to 2017 (Wu et al. 2021; Figure 1).

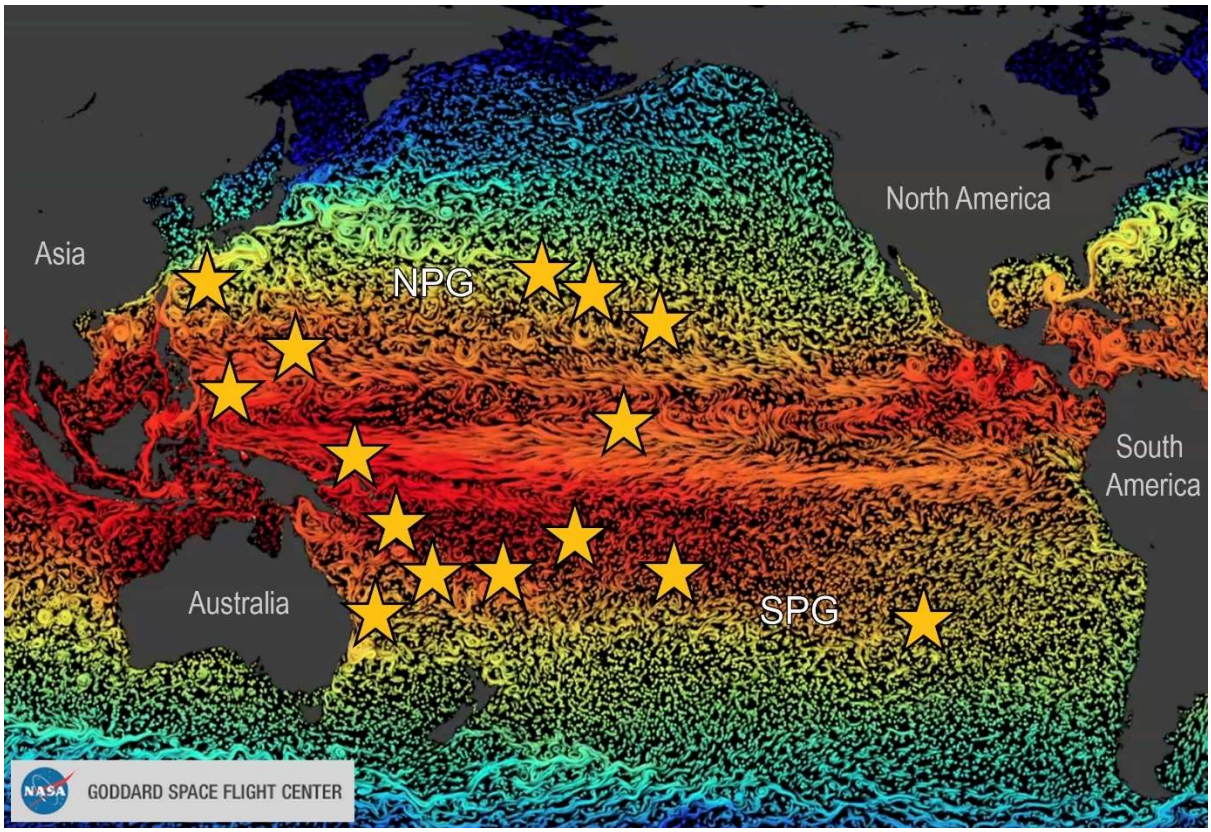

Figure 1. Locations of selected tropical and subtropical Pacific Ocean coral ^{14}C records relative to sea surface temperature (red, warmest at ~30 °C; yellow, cooler at ~16 °C) and mean current flow (line patterns in sea surface). This series of locations cover most of the region where YFT and BET of the Pacific Ocean would reside — North Pacific Gyre (NPG) to South Pacific Gyre (SPG) and across the WCPO — and exemplify the range of expected bomb ^{14}C levels for otoliths formed while living in the mixed layer of this broad region (Figure 2). Map snapshot is from NASA Perpetual Oceans – Scientific Visualization Studio (Global Sea Surface Currents and Temperature).

The collective tropical-subtropical Pacific Ocean ^{14}C reference chronology covers a geographical area that ranges northward to the Hawaiian Islands, southward to Easter Island, and across the western Pacific from the southern Great Barrier Reef to numerous locations across the western North Pacific (Figure 2). While there are constraints to potential years of formation for ^{14}C values measured in otoliths from across this broad region of the Pacific Ocean, it is the addition of yoy tuna otoliths as reference material that can provide confirmation of the temporal alignments for the ^{14}C measurements made for older aged tuna otoliths. This ^{14}C reference data set excludes records from marginal seas and regions of upwelling to avoid complications due to terrigenous influxes and mixing of ^{14}C-depleted deep-water sources and to focus on the potential range of values for pelagic waters. Radiocarbon measurements are presented as fraction modern ($F^{14}C$), values that are corrected for fractionation using $\delta^{13}C$ measured online, and in some instances as date-of-formation corrected $\Delta^{14}C$ to allow comparisons with other studies that did not report $F^{14}C$ (Reimer et al., 2004).

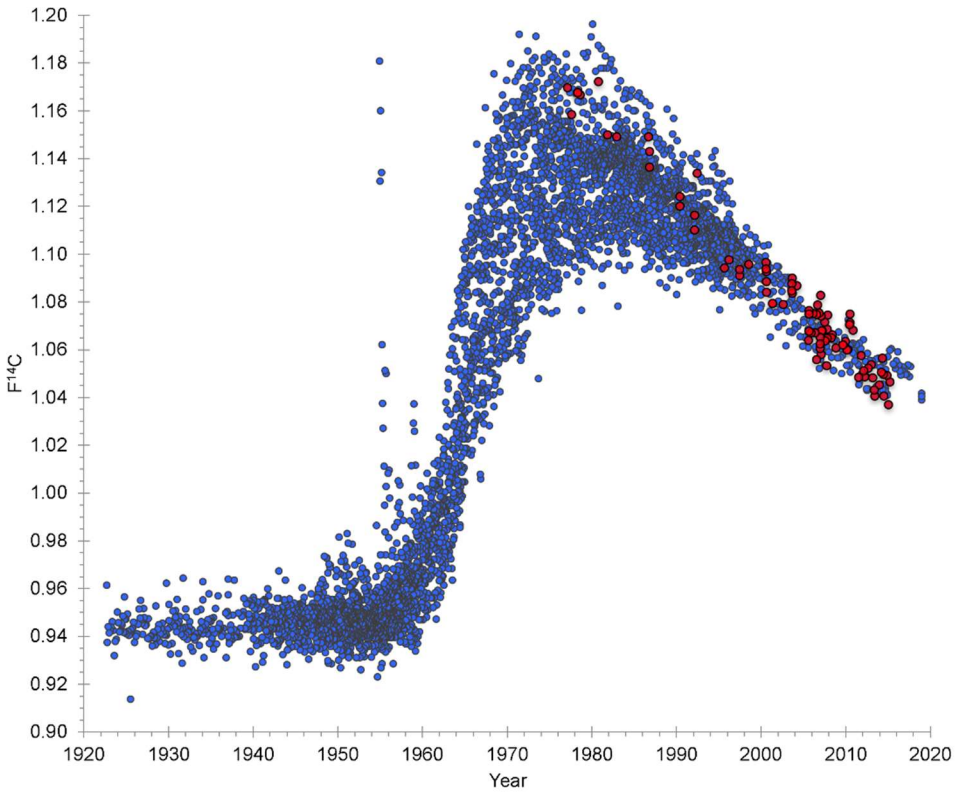

Figure 2. Plot of all known regional coral (blue) and known date-of-formation otolith (red) ^{14}C data from the tropical and subtropical Pacific Ocean that can be used as reference material. The initial ^{14}C data composition that covers numerous sources are referenced in Andrews et al. (2018). Recent coral and otolith data was added from American Samoa (Andrews et al., 2021b) and the Great Barrier Reef (Wu et al. 2021). This data set is used further, in concert with the yoy tuna otoliths measured in this study, to provide a temporal reference for measured ^{14}C values in older tuna otolith cores. The $F^{14}C$ spikes in the mid-late 1950s that deviate from the pattern are from close-in fallout ^{14}C that was documented in coral from Guam, a location that is down current from the Pacific Proving Grounds (Andrews et al. 2016).

The priority of this part of the study was careful selection of yoy otoliths to cover the post-peak ^{14}C decline period. Collections of WCPFC Pacific Marine Specimen Bank (PMSB; see SC17-RP-35b-01 for details) were fully canvased for both BET and YFT juveniles that were either previously aged with daily increment counts or were assumed to be small enough in terms of body size (<50 cm FL) to be less than 1 year old — emphasis was placed on using the smallest fish first (near 30 cm FL). The selections were expanded to include larger fish as necessitated by the desire to establish the most complete ^{14}C time series possible. A total of 134 yoy tuna otoliths provided ^{14}C measurements that covered years of otolith formation from 1989 to 2019 (Table 1). The data set was represented by 62 YFT, 54 BET, and 18 skipjack (SKJ; *Katsuwonus pelamis*). Young-of-the-year otoliths for YFT were more prevalent and therefore outnumber the selected BET yoy otoliths, and SKJ yoy otoliths were selected to fill gaps, but also out of interest to add ^{14}C measurements from a third species across the same geographic region. An existing ^{14}C data set of 29 BET yoy (previously measured in Japan) was added that covered years of formation 2010–2018 for a total of 83 BET yoy (Table 2).

The regional coverage of the available yoy tuna specimens was also a factor in considering its inclusion as a reference measurement for otolith ^{14}C. The existing BET reference series covered a geographical range of 5°N–8°S and 144°E–164°E. The latitudinal and longitudinal range was expanded for the selected otoliths of this study to cover a broader range of natal origins across the WCPO and ranged from 4°N to 21°S and 140°E to 127°W. Most yoy were from a narrower geographical range (4°N–9°S, 140°E–180°) with a few from more distant locations to the east and south to assess potential variability in ^{14}C uptake by the otolith between locations (Figure 3).

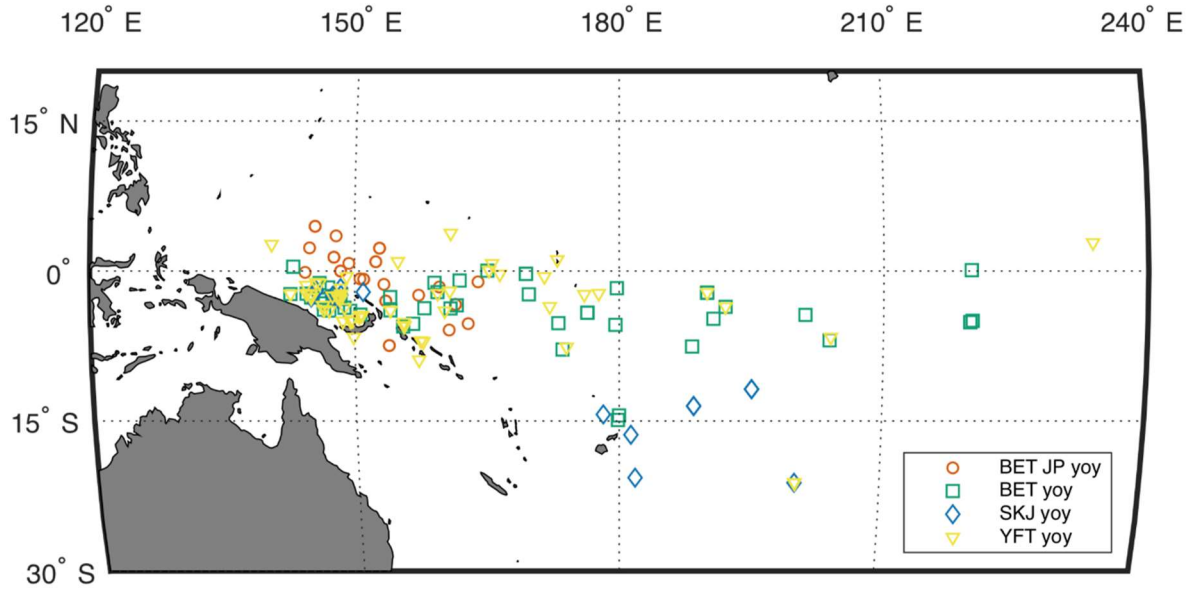

Figure 3. Distribution of yoy YFT, BET, and SKJ selected and measured in this study for the tuna ^{14}C reference chronology. The BET samples are split into those analysed in the current study and those analysed in a previous Japanese (JP) study.

Extraction of the earliest growth, similar to what was performed later for the older aged adult otoliths, was the target for measurement of ^{14}C as tuna reference material. Each otolith was prepared as described by Andrews et al. (2020). Microscopic examination of extracted otolith material, coupled with containment using a flexible mounting medium (Cytoseal 60), led to confidence that the earliest growth (within the first year of life based on daily increments observed in many of the whole otoliths) was isolated from the otolith specimens. Measured ^{14}C values from sample masses of 0.2–0.8 mg $CaCO_3$ were successful for all submitted samples (n = 134; Table 2). The ^{14}C time series from YFT, BET and SKJ yoy otoliths revealed a strong concordance with the coral-otolith ^{14}C chronology (Figure 4). The SKJ sample series were on average lower than the YFT and BET time series but were still within the 95% prediction interval of the combined datasets (see Figure 4). As a result, the measured reference ^{14}C values from all the yoy tuna were combined with the existing coral-otolith reference chronology from the tropical-subtropical Pacific Ocean to supplement gaps in the overall ^{14}C reference chronology (Figure 4). Within this composite chronology, the post-peak range for sample comparisons was selected as >1999 to move past the dovetailing of various ^{14}C peak levels across the region, leading to an overall $F^{14}C$ decline rate of –0.00256 per year ($\Delta^{14}C$ = –2.45 ‰/year; n = 439, 1999–2019).

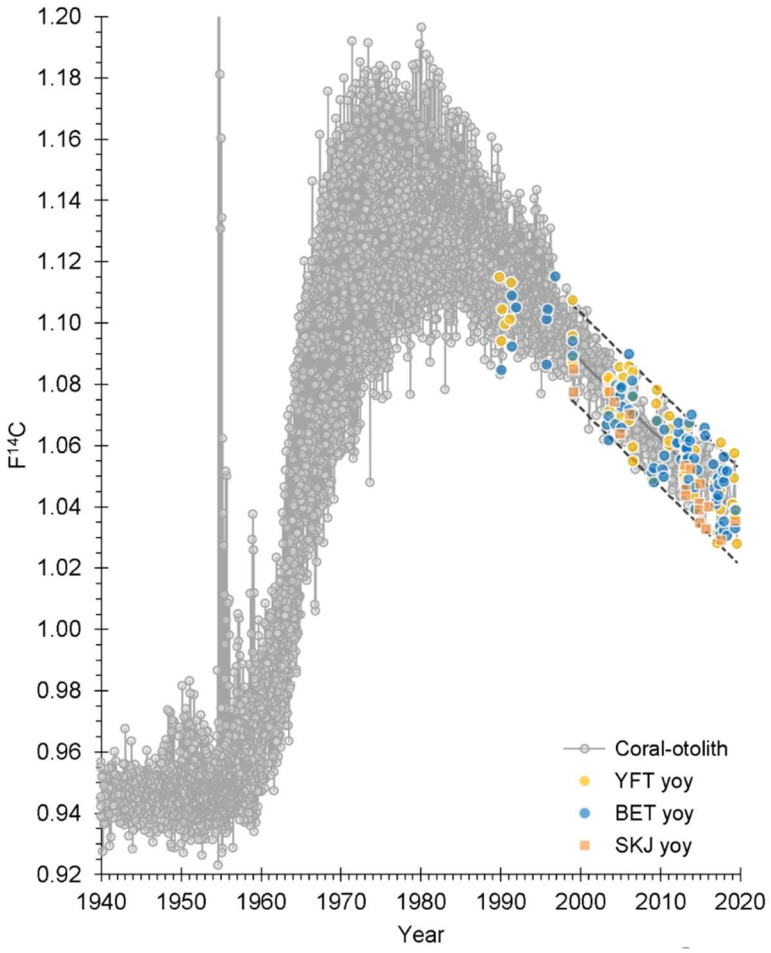

Figure 4. Plot of all ^{14}C measurements for yoy YFT, BET and SKJ across 30 years of otolith formation dates showing a strong correlation with the existing composite coral-otolith ^{14}C reference chronology. Each species demonstrated a similar post-peak relation that was strengthened by the post-peak reference chronology for use in assessing the age estimates for adult tuna from otolith core ^{14}C measurements. The years >1999 represent the common decline period among all records, including the yoy ^{14}C values from this study, across the tropical-subtropical regions of the Pacific Ocean at a rate of $F^{14}C = –0.00256$ per year ($\Delta^{14}C = –2.45‰$ per year, n = 439, 1999–2019; dashed lines = 95% prediction intervals).

Assessment of adult YFT and BET age and longevity estimates

The archives previously noted were again fully canvased for available specimens from each species that were aged and deemed most reliable with high age reading confidence. Within these selection criteria, a combination of collection year and lifespan coverage were used to focus on a series of otoliths that would effectively trace the post-peak ^{14}C decline back in time such that the slopes of the yoy ^{14}C reference series can be compared with the ^{14}C decline determined from adult otolith cores. The goal was to determine whether the decline for the older aged YFT and BET ^{14}C time series aligns with the post-peak ^{14}C decline chronology to assess the age reading protocol, an approach similar to what was successfully performed for YFT in the Gulf of Mexico (Andrews et al., 2020).

Otoliths were selected based on the above criteria, coupled with consideration of fish length and otolith mass, to select the full range of lengths and ages available for each species (see Andrews et al., (2021a) [WCPFC-SC17-2021/SA-IP-09] for details). The result was a selection of more than 150 adult tuna to cover the estimated age range of each species and across the widest range of birth years possible. From within the selected samples, 77 otoliths from older YFT aged 1–14 years and 65 otoliths from older BET aged 1–13 years were cored (earliest growth extracted) and analysed for ^{14}C levels. The geographical distribution covered by the measured ^{14}C samples is illustrated along with the overall yoy tuna reference samples for this study (Figure 5).

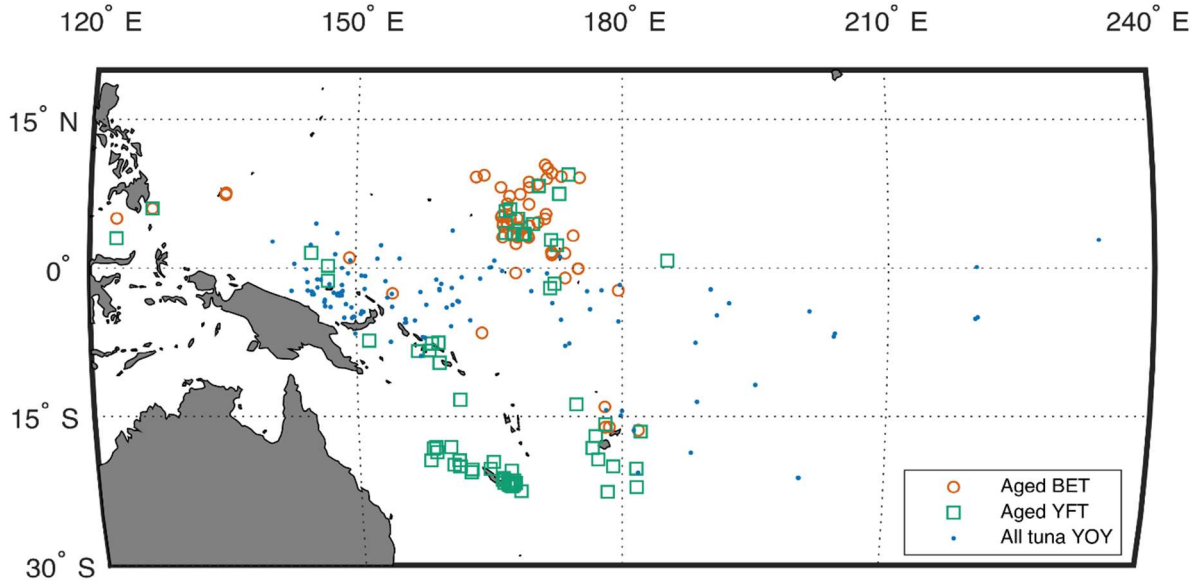

Figure 5. Distribution of collection locations for the older aged YFT and BET selected for age validation are plotted along with the yoy tuna ^{14}C reference chronology locations (Figure 3).

The alignment of the older aged YFT ^{14}C measurements with the coral-otolith reference chronology — including all yoy tuna otoliths measured in this study — corroborates the age estimates and age reading protocol to 14 years (Figure 6a). Of the 76 measured ^{14}C values (one sample was not measurable, Table 3), only four clearly reside outside the expected birth years established by the ^{14}C reference chronology (95% prediction intervals, PI). One value was lower than can be accounted for by the variability in otolith uptake and may be attributed to either over-estimated age by at least 3 years (aged to 11.2 years but may have been less than 8 years old) or an inadvertent inclusion of newer (more recently formed) otolith material during the core extraction process. When considering the overall agreement of the other older aged fish and the otolith mass of this specimen (2014Y-145, 0.1056 g) — a reasonable proxy for age (Andrews et al. 2021a) —it is likely there was a problem with the sample composition as opposed to age estimation. Three other values were similarly offset but to greater ^{14}C values. The two most elevated would need to be 3 to 5 years older to begin to align with the PI of reference chronology (aged 3.3 years but would need to be 6–7 years old, and aged 9.7 years but would need to be 14–15 years old, respectively). The sample with the greatest offset would need to be 6 years older than the estimated age of ~1.2 years, which is unlikely for a 79 cm FL fish. Hence, it is likely that there was a problem with the sample or ^{14}C measurement that led to these offset values, as opposed to a problem with underestimated age. Several other samples along the upper margin may have been 1-2 years older than the age estimates but measurement error ($F^{14}C$ ±0.007) encompasses the expected range as designated by the 95% PI. Even though there were a few outliers, the coincidence of the data sets for the 72 ^{14}C measurements (excluding outliers) aged 1–14 years, with similar decline slopes between the YFT and the coral-otolith chronology ($F^{14}C$ rate = –0.00200 *cf.* –0.00265 per year, $\Delta^{14}C$ rate = –1.88 *cf.* –2.54 ‰ per year), for the decline period established by the YFT birth years (2000–2015, $t_{0.05(2),406}$ = 1.966, t_{crit} = 1.706; P = 0.0888) provides support for the age estimates. If there was a consistent bias in the age estimates, for example, if growth bands were deposited more (or less) frequently than annual, then the ^{14}C decline curve for the YFT validation samples would be shifted to the left (right) of the reference curve. To test for such a bias, a linear regression model was fit to the reference and YFT validation data sets, assuming a common slope but allowing for the intercepts to differ (Figure 6b). No significant difference was found between the intercepts (difference of 0.0014 per year; t-value = 1.286, df = 492, P = 0.199), indicating that the age estimates are not significantly biased. However, small biases in the age estimates, due to say over or undercounting in the earliest otolith growth structure, would not

necessarily be detected as significantly different intercepts given the large variability in the ^{14}C values. Thus, an age estimate bias analysis was conducted whereby the age estimates were intentionally biased by -1, -0.5, 0, +0.5, +1 years to determine which value minimized the sum of squared residuals (SSR; Kastelle et al. 2008) between the $F^{14}C$ reference chronology and the YFT $F^{14}C$ values using the YFT adjusted birth years. This analysis revealed age estimates were accurate within a minor bias of –0.5 years (number of intentionally biased years (SSR value): –1 (697), –0.5 (693), 0 (726), +0.5 (794), +1 (898)).

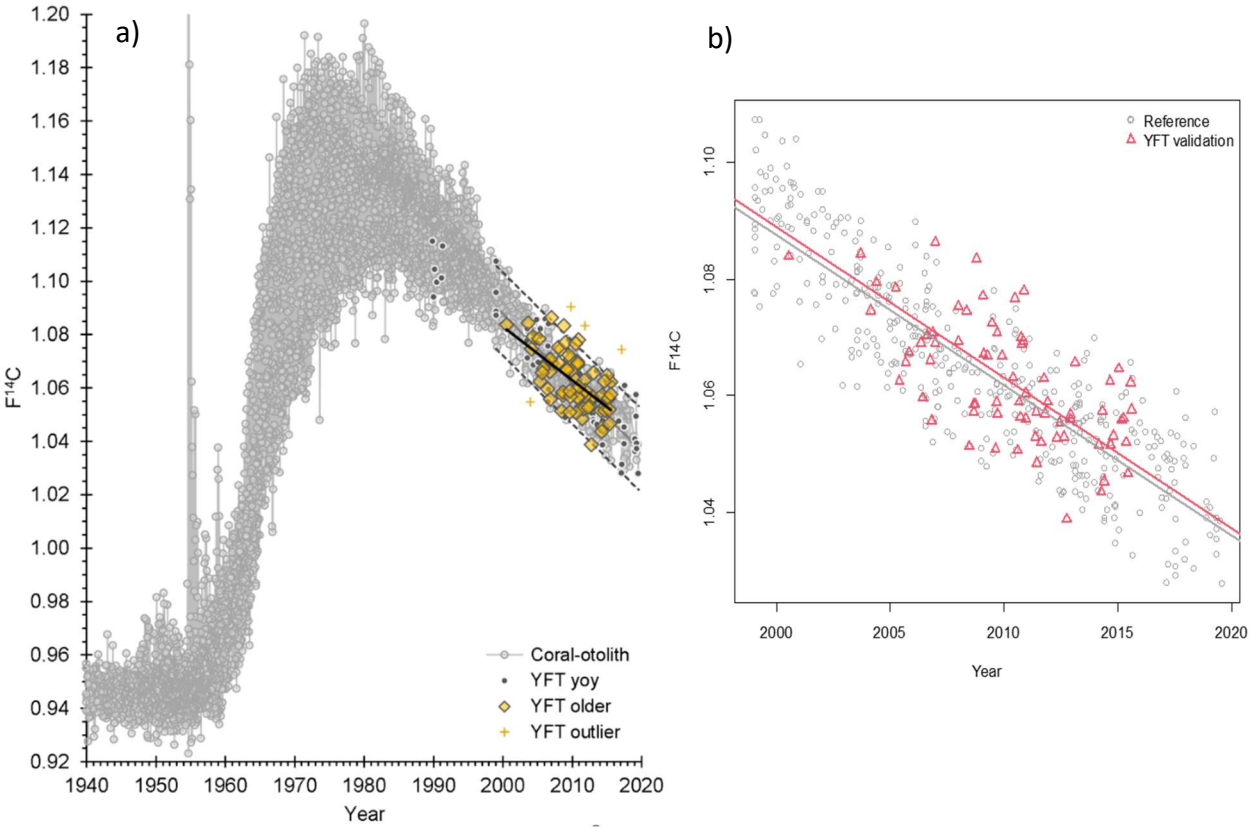

Figure 6. (a) Plot of otolith ^{14}C data for older aged YFT and regional coral-otolith reference chronologies with yoy YFT highlighted within the new comprehensive reference chronology. The ^{14}C measurements from older (validation) YFT aged 1–14 years were in alignment with the coral-otolith reference series, exhibiting similar decline rates and spatial-temporal concordance. The years >1999 represent the common decline period among all coral-otolith records (including all yoy tuna) at a rate of –2.45‰ per year (dashed lines = 95% prediction intervals, PI), similar to the regression of older aged YFT at –1.88‰ per year (thick black line). Of the 76 successful otolith core measurements, only four were considered outliers as indicated by the 95% PI. Hence, the series of birth years derived from age reading of thin-sectioned otoliths are well supported through ontogeny. (b) Linear regression model fitted to the comprehensive reference and YFT validation ^{14}C data sets for years >1999, assuming a common slope but allowing for different intercepts. The intercepts were not significantly different (*t*-value = 1.286, *df* = 492, *P* = 0.199), indicating there is no significant bias in the age estimates.

The alignment of the older aged BET ^{14}C measurements with the coral-otolith reference chronology — including the yoy tuna otoliths measured in this study — corroborated the age estimates and age reading protocol to 13 years (Figure 7a). Of the 64 measured ^{14}C values (one sample was lost, Table 4), no specimens clearly resided outside the expected birth years established by the ^{14}C reference chronology (95% PI). Two measurements were marginally lower than expected, but the overall trend supports the otolith age reading interpretations from thin-sectioned otoliths. The coincidence of the data sets for the ^{14}C measurements, with similar decline slopes between the older aged BET and coral-otolith chronologies ($F^{14}C$ rate = –0.00249 cf. –0.00260 per year, $\Delta^{14}C$ rate = –2.38 cf. –2.49 ‰ per year), for the decline period established by the BET birth years (2002–2015, $t_{0.05(2),353}$ = 1.967, t_{crit}

= 1.167; *P* = 0.2440) provides support for the age estimates through ontogeny. A linear regression model fitted to the reference and BET validation data sets assuming a common slope, but different intercepts revealed no bias in the age estimates (Figure 7b; difference in intercepts of -0.0016 per year; *t*-value = -1.483, *df* = 484, *P* = 0.139). Furthermore, an age estimate bias analysis using the BET birth years relative to the $F^{14}C$ reference chronology by minimizing the sum of squared residuals (SSR; Kastelle et al. 2008) revealed age estimates were accurate with no bias (number of intentionally biased years (SSR value): –1 (562), –0.5 (504), ***0 (477)***, +0.5 (481), +1 (516)).

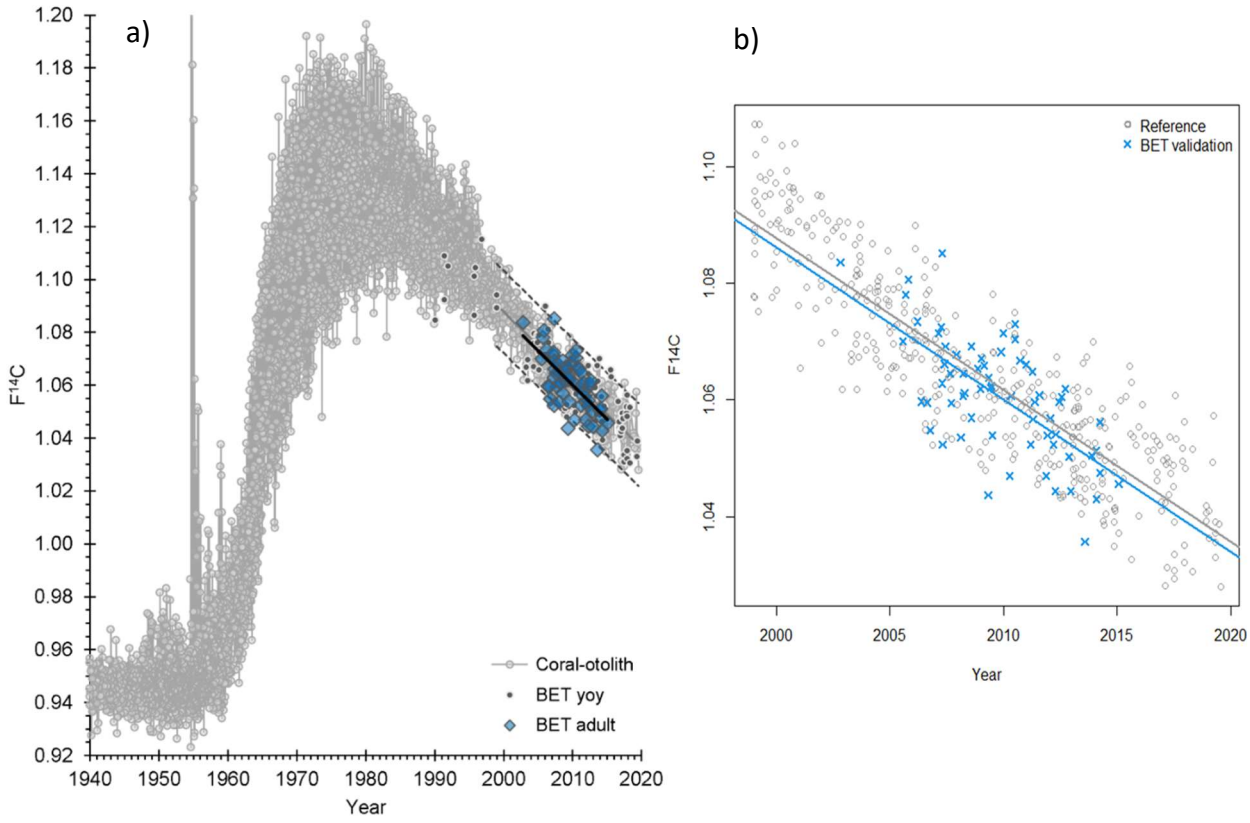

Figure 7. (a) Plot of otolith ^{14}C data for older aged BET with yoy BET and regional coral-otolith reference chronologies with yoy BET highlighted within the new comprehensive reference chronology. The ^{14}C measurements from older (validation) BET aged 1–13 years were in alignment with the coral-otolith reference series, exhibiting similar decline rates and spatial-temporal concordance. The years >1999 represent the common decline period among all coral-otolith records (including all yoy tuna) at a rate of –2.45‰ per year (dashed lines = 95% prediction intervals, PI), similar to the regression of older aged BET at –2.38‰ per year (thick black line). The 64 successful otolith core measurements provide a series of birth years, derived from age reading of thin-sectioned otoliths, that are well supported through ontogeny. (b) Linear regression model fitted to the comprehensive reference and BET validation ^{14}C data sets for years >1999, assuming a common slope but allowing for different intercepts. The intercepts were not significantly different (*t*-value = -1.483, *df* = 484, *P* = 0.139), indicating there is no significant bias in the age estimates.

Juvenile-to-adult radiocarbon uptake

Laser ablation accelerator mass spectrometry (LA-AMS) technology uses a new apparatus that is being developed by researchers at ETH Zürich to provide continuous measurement of ^{14}C across geologic and biogenic carbonates (Welte et al., 2016). The original plan for the current study was to analyse BET otoliths from several large adults with the most massive otoliths and greatest age estimates to document changes in ^{14}C uptake that may be attributed to residing at greater depths through ontogeny. However, the consensus was that the otoliths of tuna are too small to provide meaningful results from the LA-AMS system. The reasons were due to the following limitations: 1) the otoliths do not exhibit a growth structure that would facilitate a good linear scan with enough depth and width along an age-specific pathway, and 2) preparation of planar sections that contain

sufficient material would not be possible based on the required dimensions for laser scanning. While this approach was successful in providing complete bomb ^{14}C signals through ontogeny for the massive otoliths (up to 5 g) of red snapper (*Lutjanus campechanus*; Andrews et al. 2019), the technology currently does not have the resolution to analyse the small otoliths of tuna (typically less than 0.2 g). Hence, it was concluded that the next best approach was to analyse an additional sample from the rostrum tip from a series of the oldest aged fish with the most massive otoliths to allow a comparison of ^{14}C uptake between earliest and latest otolith growth.

Several otoliths of the oldest YFT and BET were selected for additional otolith sampling of the rostrum tip to provide a potential contrast in ^{14}C uptake between species. Rostrum tip sampling was not possible for all of the oldest specimens because this part of the otolith was missing in some cases. The ages and otolith masses that were sampled covered 8–13 years (n = 9; 0.1026–0.1230 g) for YFT and 7–10 years (n = 11; 0.0849–0.1235 g) for BET (Tables 5 and 6). It is estimated that ~3 years of otolith growth was removed when the rostrum tip was sampled manually based on microscopic observations. Hence, the period between birth year otolith formation (core adjusted by 0.5 years) and the capture date for the measured ^{14}C values was adjusted by 1.5 years, leading to calculated time spans of 6.5–10.9 years for YFT and 4.6–7.7 years for BET. Most core-tip sample sets for these large tuna specimens began at an elevated ^{14}C level and decreased as expected with increasing age, but some either changed little or were more elevated at the rostrum tip (Figure 8). The YFT core-tip sample series begins by covering the range of ^{14}C values expected from the coral-otolith reference chronology and ends on the upper edge, but still mostly within the expected decline distribution. Three of the oldest fish (10–13 years) decline strongly, three changed little but resided within the expected distribution, and two were outliers with values that exceed the reference chronology and cannot be explained (likely anomalous values due to handling or unusual measurement problems). A recent ^{14}C chronology from a coral core of Masthead Reef on the southern end of the Great Barrier Reef (Wu et al. 2021) reveals an alignment with the rostrum tip samples for some of the YFT, which is consistent with New Caledonia as the collection location for these specimens — Coral Sea ^{14}C levels cross this region via the South Equatorial Current (Andrews et al., 2016, 2021; Wu et al., 2021). The BET core-tip sample series covers the range of ^{14}C values expected from the reference chronology from beginning to end, except for one outlier that is ^{14}C-depleted. These specimens cover a wide range of collection locations in terms of latitude-longitude and the depleted sample does not stand out geographically. Because BET is known as a vertical migrator in the mixed layer of the water column, especially with increasing size and age (Brill et al., 2005; Evans et al., 2008; Houssard et al., 2017), the alignment within the range of potential ^{14}C values for the mixed layer is consistent with these observations. It is possible that the ^{14}C-depleted individual may have been a fish with greater residence times in deeper ^{14}C-depleted waters during the last few years of its life.

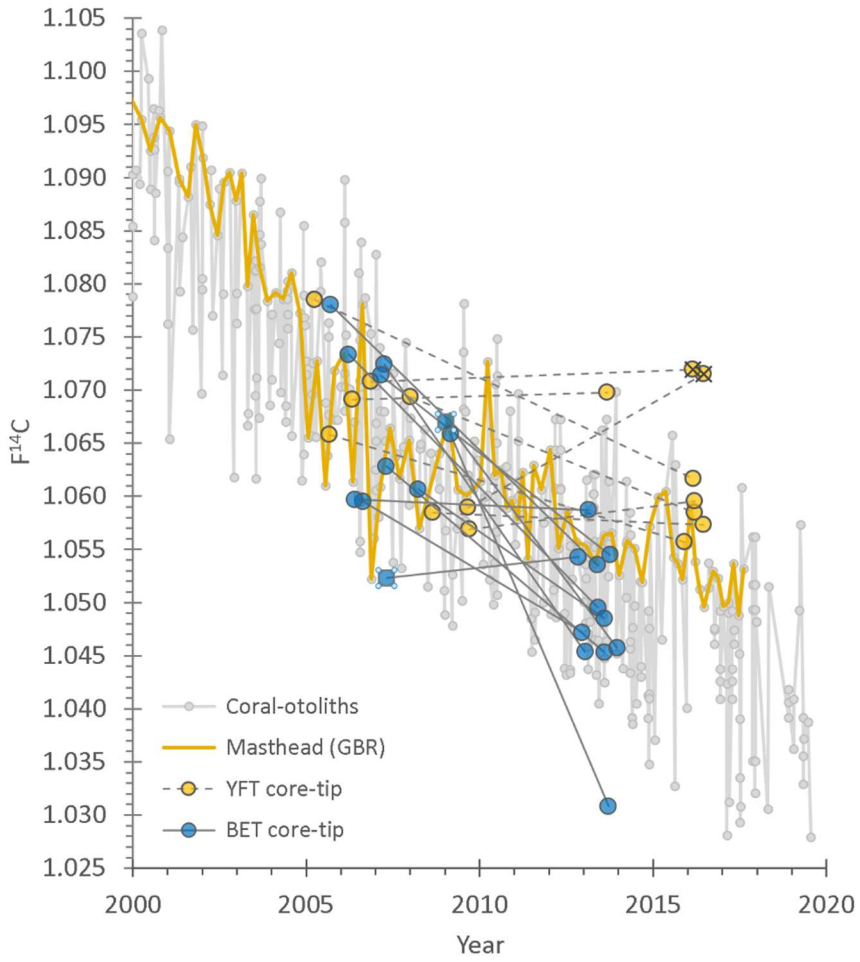

Figure 8. Plot of otolith ^{14}C data for otolith core and tip of the rostrum samples from a few of the largest and oldest YFT and BET specimens as an indication of ^{14}C uptake from the juvenile otolith core to the last few years as an adult for the capture waters (Tables 5 and 6). Included is an emphasis on a coral chronology from Masthead Reef on the Great Barrier Reef (GBR; Wu et al. 2021) that is likely to represent the YFT capture waters of New Caledonia. Outlier YFT tip samples are noted with an X because there is no clear explanation as to why they are elevated — deviation from the expected coral-otolith chronology is slightly greater than the measurement error (mean = ±0.0070). Overall, the expected ^{14}C decline through ontogeny is well represented for older aged YFT and BET.

Age estimates and the oldest groups

The alignment of ^{14}C values generated by the birth year material of aged YFT and BET over all age classes within the post-peak bomb ^{14}C decline corroborates the age reading of annual growth zones in thin sectioned otoliths. While individual ages cannot be determined directly from the ^{14}C reference chronology due to the margin of uncertainty associated with the decline time series, the age of some fish can be constrained by the 95% PI limits. For YFT, two individuals aged as 8.8 years (2018Y-150B) and 10.4 years (2018Y-148) were unlikely to be less than 9 years old from the PI limits. These fish measured 148 cm and 150 cm straight fork length (SFL) with elevated $F^{14}C$ values of 1.0767 and 1.0791, respectively. The oldest aged YFT of 13.8 years was more centrally located among others aged 10 years and older, exhibiting a range of ^{14}C values that cover the expected distribution for the calculated birth years (Figure 9). An empirical test for alignment of the oldest fish as a group with what is predicted from the coral-otolith chronology revealed a close agreement between mean estimated age and the predicted mean age from the post-peak decline regression. This group of oldest YFT cover 9.8 to 13.8 years with a mean estimated age of 11.2 years (n = 12, collection years 2013–2018). The mean ^{14}C value from the measured otolith cores for this group was calculated as $F^{14}C$ = 1.0737 (range 1.0585–1.0843), which leads to a mean predicted birth year from

the coral-otolith chronology of 2005.45 ($F^{14}C$ = –0.002565*year + 6.2185). Hence, the mean age for this group was 11.1 years (based on a mean collection date of 2016.52 for the group), effectively in agreement with the mean estimated age of the group. Because the YFT covered more than just a few collection years (5-year period), the group was also split into two collection years sub-groups of 2013–2014 (n = 4) and 2016–2018 (n = 8), leading to similar results for the age prediction comparisons (11.6 *cf.* 11.5 years and 11.0 *cf.* 10.9 years, respectively).

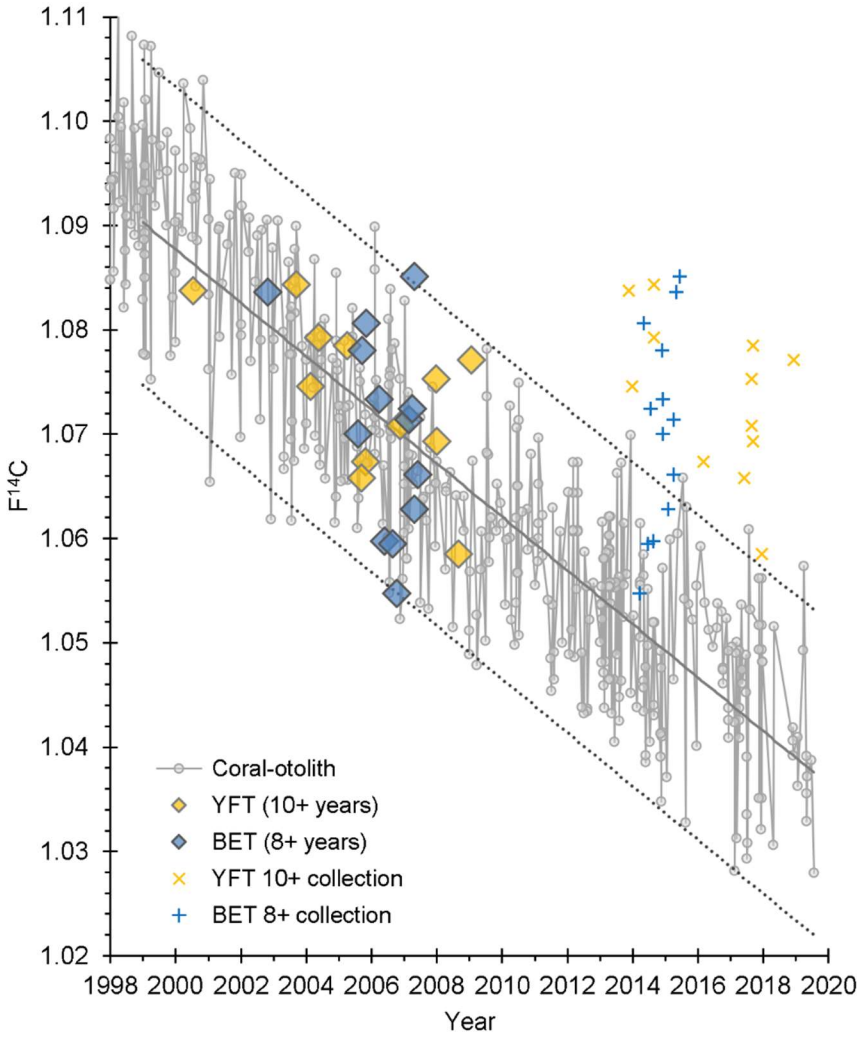

Figure 9. Plot of otolith ^{14}C data for the oldest age groups as an empirical demonstration of older ages based entirely on support from mean measured ^{14}C values. Given the original specimen collections were made within a narrow period of time, it is expected that the mean estimated age would generate a mean birth year that is similar to what is predicted by the post-peak decline $F^{14}C$ value.

This approach is similar to geochemical methods that use pooled samples to achieve enough measurable activity between two radionuclides in disequilibrium. For example, lead-210:radium-226 dating uses a collection of otolith cores from fish with similar ages into groups to either support or refute the age reading (e.g., orange roughy, *Hoplostethus atlanticus*; Andrews et al. (2009) and opakapaka, *Pristipomoides filamentosus*; Andrews et al. (2012)). The method is typically used for species that live several decades to ages approaching or exceeding 100 years but has also been used to determine that Pacific cod (*Gadus macrocephalus*) live no more than 10–12 years (Andrews 2016). For the collection of 12 YFT individuals aged 10–14 years, a mean radiocarbon age of 11.1 years is an indication that the lifespan of YFT in the WCPO exceeds 11 years.

For BET, an individual measuring 137 cm SFL was aged to 8.6 years provided a core $F^{14}C$ value of 1.0836 (2015B-137). Based on the calculated birth year of 2007 and the 95% PI, this fish is unlikely to have been younger. The oldest BET aged 13 years is more centrally located in time within the potential range of ^{14}C values and the range of fish older than 8 years all cluster around the central tendency of the reference chronology (Figure 9). Performing the same empirical test for alignment of the oldest BET group with the coral-otolith chronology also revealed a close agreement between mean estimated age and the predicted mean age from the post-peak decline regression. This group of oldest BET cover 7.8 to 13.8 years with a mean estimated age of 9.1 years (n = 13, collection years 2014–2015). The mean ^{14}C value from the measured otolith cores for this group was calculated as $F^{14}C = 1.0712$ (range 1.0548–1.0851), which leads to a predicted mean birth year from the coral-otolith chronology of 2006.42 ($F^{14}C = –0.002565*year + 6.2185$). Hence, the mean age for this group was 8.4 years (based on a mean collection date of 2014.85 for the group), similar to the mean estimated age of the group (9.1 *cf*. 8.4 years). There was no reason to split the older aged BET group, as was the case for the older aged YFT group, because collections covered just two consecutive years. As with the YFT findings, the mean radiocarbon age of 8.4 years is an indication that the lifespan of BET in the WCPO exceeds 8 years.

In general, more fish with higher age estimates may have strengthened the relationship of maximum age relative to the coral-otolith reference chronology. While it is recommended that additional specimens with the most massive otoliths be analysed for age in thin sections and otolith core ^{14}C values to better assess maximum age, it is clear from these findings that each species is being aged using an accurate annual age reading protocol, and that a teenage lifespan is being taken more seriously in global tuna stock assessments (Horswill et al., 2019; Hoyle et al. 2023).

6. References

Andrews, A.H. (2016) Lead-radium dating of Pacific cod (*Gadus macrocephalus*) – validation of the young-fish scenario. *Marine and Freshwater Research* 67: 1982–1986 (dx.doi.org/10.1071/MF15228)

Andrews, A.H. (2020) Giant trevally (*Caranx ignobilis*) of Hawaiian Islands can live 25 years. *Marine and Freshwater Research* 71: 1367–1372 (dx.doi.org/10.1071/MF19385)

Andrews, A.H., and Scofield, T.R. (2021) Early overcounting in otoliths: a case study of age and growth of gindai (*Pristipomoides zonatus*) using bomb ^{14}C dating. *Fisheries and Aquatic Sciences* 24: 53–62 (dx.doi.org/10.47853/FAS.2021.e6)

Andrews, A.H., Tracey, D.M., and Dunn, M.R. (2009) Lead–radium dating of orange roughy (*Hoplostethus altanticus*): validation of a centenarian life span. *Canadian Journal of Fisheries and Aquatic Sciences* 66: 1130–1140 (dx.doi.org/10.1139/F09-059)

Andrews, A.H., DeMartini, E.E., Brodziak, J., Nichols, R.S., and Humphreys, R.L. (2012) A long–lived life history for a tropical, deep–water snapper (*Pristipomoides filamentosus*): bomb radiocarbon and lead–radium dating as extensions of daily increment analyses in otoliths. *Canadian Journal of Fisheries and Aquatic Sciences* 69: 1850–1869 (dx.doi.org/10.1139/f2012-109)

Andrews, A.H., Barnett, B.K., Allman, R.J., Moyer, R.P., and Trowbridge, H.D. (2013) Great longevity of speckled hind (*Epinephelus drummondhayi*), a deep-water grouper, with novel use of postbomb radiocarbon dating in the Gulf of Mexico. *Canadian Journal of Fisheries and Aquatic Sciences* 70(8): 1131–1140 (dx.doi.org/10.1139/cjfas-2012-0537)

Andrews, A.H., Choat, J.H., Hamilton, R.J., and DeMartini, E.E. (2015) Refined bomb radiocarbon dating of two iconic fishes of the Great Barrier Reef. *Marine and Freshwater Research* 66: 305–316 (dx.doi.org/10.1071/MF14086)

Andrews, A.H., Asami, R., Iryu, Y., Kobayashi, D.R., and Camacho, F. (2016) Bomb-produced radiocarbon in the western tropical Pacific Ocean—Guam coral reveals operation-specific signals from the Pacific Proving Grounds. *Journal of Geophysical Research – Oceans* 121: 6351–6366

Andrews, A.H., Humphreys, R.L., and Sampaga, J.D. (2018) Blue marlin (*Makaira nigricans*) longevity estimates confirmed with bomb radiocarbon dating. *Canadian Journal of Fisheries and Aquatic Sciences* 75: 17–25 (dx.doi.org/10.1139/cjfas-2017-0031)

Andrews, A.H., Yeman, C., Welte, C., Hattendorf, B., Wacker, L., and Christl, M. (2019) Laser ablation AMS reveals complete bomb ^{14}C signal in an otolith with confirmation of 60-year longevity for red snapper (*Lutjanus campechanus*). *Marine and Freshwater Research* 70: 1768–1780 (dx.doi.org/10.1071/MF18265)

Andrews, A.H., Pacicco, A., Allman, R., Falterman, B.J., Lang, E.T., and Golet, W. (2020) Validated longevity of yellowfin (*Thunnus albacares*) and bigeye (*Thunnus obesus*) tuna of the northwestern Atlantic Ocean. *Canadian Journal of Fisheries and Aquatic Sciences* 77: 637–643 (dx.doi.org/10.1139/cjfas-2019-0328)

Andrews, A., Okamoto, K., Satoh, K., Roupsard, F., and Farley, J. (2021a) Progress report on bomb radiocarbon age validation for bigeye and yellowfin tunas in the WCPO (Project 105). SCIENTIFIC COMMITTEE SEVENTEENTH REGULAR SESSION (Electronic Meeting 11–19 August 2021), WCPFC-SC17-2021/SA-IP-09 [https://meetings.wcpfc.int/node/12567]

Andrews, A.H., Prouty, N.G., and Cheriton, O.M. (2021b) Bomb-produced radiocarbon across the South Pacific Gyre – a new record from American Samoa with utility for fisheries science. *Radiocarbon* 63: 1591–1605 (dx.doi.org/10.1017/RDC.2021.51)

Brill, R.W., Bigelow, K.A., Musyl, M.K., Fritsches, K.A., Warrant, E.J. (2005) Bigeye tuna (*Thunnus obeus*) behavior and physiology and their relevance to stock assessments and fishery biology. *ICCAT Collective Volume of Scientific Papers* 57: 142–161

Campana, S.E. (1999) Chemistry and composition of fish otoliths: pathways, mechanisms and applications. Marine Ecological Progress Series 188: 263–297

Ducharme-Barth, N., Vincent, M., Hampton, J., Hamer, P., Williams, P. and Pilling, G. (2020) Stock assessment of bigeye tuna in the western and central Pacific Ocean. SC16/SA-WP-03. Sixteenth Regular Session of the Scientific Committee of the Western and Central Pacific Fisheries Commission. Online meeting, 11–20 August 2020.

Evans, K., Langley, A., Clear, N.P., Williams, P., Patterson, T., Sibert, J., Hampton, J., and Gunn, J.S. (2008) Behaviour and habitat preferences of bigeye tuna (*Thunnus obesus*) and their influence on longline fishery catches in the western Coral Sea. *Canadian Journal of Fisheries and Aquatic Sciences* 65: 2427–2443

Farley, J.H., Clear, N.P., Leroy, B., Davis, T.L.O., and McPherson, G. (2006) Age, growth and preliminary estimates of maturity of bigeye tuna, *Thunnus obesus*, in the Australian region. Marine and Freshwater Research 57: 713–724

Farley, J., Eveson, P., Krusic-Golub, K., Clear, N., Sanchez, C., Roupsard, F., Satoh, K., Smith, N., and Hampton, J. (2018) Update of bigeye age and growth in the WCPO. WCPFC Project 81. WCPFC-SC14-2018/SA-WP-01, Busan, Republic of Korea, 8–16 August 2018.

Farley, J., Krusic-Golub, K., Clear, N., Eveson, P., Smith, N., and Hampton, J. (2019) Project 94: Workshop on yellowfin and bigeye age and growth. WCPFC-SC15-2019/SA-WP-02, Pohnpei, Federated States of Micronesia, 12–20 August 2019.

Farley, J., Andrews, A., Clear, N., Hampton, J., Ishihara, T., Krusic-Golub, K., MacDonald, J., Okamoto, K., Satoh, K., and Williams, A. (2020a) Report on the bomb radiocarbon age validation workshop for tuna and billfish in the WCPO. WCPFC-SC16-2020/SA-IP-17. Online, 11–20 August 2020.

Farley, J., Krusic-Golub, K., Eveson, P., Clear, N., Roupsard, F., Sanchez, C., Nicol, S., and Hampton, J. (2020b) Age and growth of yellowfin and bigeye tuna in the western and central Pacific Ocean from otoliths. WCPFC-SC-16-2020/SC16-SA-WP-02, Online, 11–20 August 2020.

Griffiths, S.P., Fry, G.C., Manson, F.J., and Lou, D.C. (2010) Age and growth of longtail tuna (*Thunnus tonggol*) in tropical and temperate waters of the central Indo-Pacific. *ICES Journal of Marine Science* 67: 125–134

Hamer, P, and Pilling, G. (2020) Report from the SPC pre-assessment E-workshop, Noumea, April 2020. WCPFC-SC16-2020/SA-IP-02

Horswill, C., Kindsvater, H.K., Juan-Jordá, M.J., Dulvy, N.K., Mangel, M., and Matthiopoulos, J. (2018) Global reconstruction of life-history strategies: A case study using tunas. *Journal of Applied Ecology* 56: 855–865

Hoyle, S.D., Williams, A.J., Minte-Vera, C.V., and Maunder, M.N. (2023) Approaches for estimating natural mortality in tuna stock assessments: Application to global yellowfin tuna stocks. *Fisheries Research* 257: 1006489 (dx.doi.org/10.1016/j.fishres.2022.106498)

Ishihara, T., Abe, O., Shimose, T., Takeuchi, Y., and Aires-da-Silva, A. (2017) Use of postbomb radiocarbon dating to validate estimated ages of Pacific bluefin tuna, *Thunnus orientalis*, of the North Pacific Ocean. *Fisheries Research* 189: 35–41

Houssard, P., Lorrain, A., Tremblay-Boyer, L., Allain, V., Graham, B.S., Menkes, C.E., Pethybridge H., Couturier, L.I.E., Point, D., Leroy, B., Receveur, A., Hunt, B.P.V., Vourey, E., Bonnet, S., Rodier, M., Raimbault, P., Feunteun, E., Kuhnert, P.M., Munaron, J.-M., Lebreton, B., Otake, T., and Letourneur, Y. (2017) Trophic position increases with thermocline depth in yellowfin and bigeye tuna across the Western and Central Pacific Ocean. *Progress in Oceanography* 154: 49–63

Ishihara, T., Abe, O., Shimose, T, Takeuchi, Y., and Aires-da-Silva, A. (2017) Use of post-bomb radiocarbon dating to validate estimated ages of Pacific bluefin tuna, *Thunnus orientalis*, of the North Pacific Ocean. *Fisheries Research* 189: 35–41

Kalish, J.M. (1993) Pre- and pot-bomb radiocarbon in fish otoliths. *Earth and Planetary Science Letters* 114: 549–554

McKechnie, S., Pilling, G., and Hampton, J. (2017) Stock assessment of bigeye tuna in the western and central Pacific Ocean. WCPFC-SC13-2017/SA-WP-05. Rarotonga, Cook Islands 9–17 August 2017.

Reimer, P.J., Brown, T.A., and Reimer, R.W. (2004) Discussion: Reporting and calibration of post-bomb ^{14}C data. *Radiocarbon* 46: 1299–1304

SPC-OFP (2021) Project 35b: WCPFC Tuna Tissue Bank. WCPFC-SC17-2021/RP-P35b-01. Sixteenth Regular Session of the Scientific Committee of the Western and Central Pacific Fisheries Commission. Online meeting, 11-19 August 2021.

Vincent, M.T., Pilling, G.M., and Hampton, J. (2018) Incorporation of updated growth information within the 2017 WCPO bigeye stock assessment grid, and examination of the sensitivity of estimates to alternative model spatial structures. WCPFC-SC14-2018/ SA-WP-03. Busan, Republic of Korea 8–16 August 2018.

Welte, C., Wacker, L., Hattendorf, B., Christl, M., Fohlmeister, J., Breitenbach, S.F.M., Robinson, L.F., Andrews, A.H., Freiwald, A., Farmer, J.R., Yeman, C., Synal, H.-A., and Günther, D. (2016) Laser Ablation – Accelerator Mass Spectrometry: a novel approach for rapid radiocarbon analyses of carbonate archives at high spatial resolution. *Analytical Chemistry* 88: 8570–8576

Williams, A.J., Leroy, B.M., Nicol, S.J., Farley, J.H., Clear, N.P., Krusic-Golub, K., and Davies, C.R. (2013) Comparison of daily- and annual-increment counts in otoliths of bigeye (*Thunnus obesus*), yellowfin (*T. albacares*), southern bluefin (*T. maccoyii*) and albacore (*T. alalunga*) tuna. *ICES Journal of Marine Science* 70: 1439–1450

Wu, Y., Fallon, S.J., Cantin, N.E., and Lough, J.M. (2021) Surface ocean radiocarbon from Porites coral record in the Great Barrier Reef: 1945–2017. *Radiocarbon* 63: 1193–1203

Table 1. Fish and otolith information with corresponding ^{14}C data for the 134 young-of-the-year tuna specimens that were selected as reference material. Lab number reflects collection year and species (Y=YFT, B=BET, S=SKJ) and the details number includes longitude and EEZ ID. Fish length is provided as straight fork length (SFL) in mm with the capture date. Radiocarbon measurements are listed as $F^{14}C$ with instrument measurement error and as formation-date-corrected $\Delta^{14}C$ in per mille (Reimer et al. 2004).

Lab number	Detailed number	SFL (mm)	Capture date	$F^{14}C$	Err (abs)	$\Delta^{14}C$ (‰)
1990B-1	1990B-154-PG	470	25-Apr-1990	1.0846	0.0079	79.3
1990Y-1	1990Y-202-I7	440	9-Feb-1990	1.1149	0.0067	109.5
1990Y-2	1990Y-172-GL	410	11-Oct-1990	1.0994	0.0077	94.0
1990Y-3	1990Y-154-PG	320	25-Apr-1990	1.0941	0.0079	88.8
1990Y-4	1990Y-144-PG	290	15-Jun-1990	1.1044	0.0066	99.1
1991B-1	1991B-169-GL	370	15-Sep-1991	1.0923	0.0079	86.8
1991B-2	1991B-169-GL	320	15-Sep-1991	1.1088	0.0080	103.3
1991Y-1	1991Y-154-FM	500	2-Aug-1991	1.1131	0.0070	107.5
1991Y-2	1991Y-155-PG	300	15-Jun-1991	1.1010	0.0066	95.6
1992B-1	1992B-179-GL	490	31-Mar-1992	1.1049	0.0080	99.3
1996B-1	1996B-220-PF	480	2-Mar-1996	1.1045	0.0079	98.4
1996B-2	1996B-219-PF	470	18-Jan-1996	1.1012	0.0078	95.1
1996B-3	1996B-219-PF	460	18-Jan-1996	1.0864	0.0078	80.4
1997B-1	1997B-220-PF	460	12-Feb-1997	1.1152	0.0078	108.9
1999B-1	1999B-144-PG	500	23-Apr-1999	1.0940	0.0077	87.5
1999B-2	1999B-144-PG	450	18-Apr-1999	1.0893	0.0076	82.8
1999S-1	1999S-148-PG	320	26-Apr-1999	1.0776	0.0075	71.2
1999S-2	1999S-145-PG	300	20-Apr-1999	1.0850	0.0076	78.6
1999Y-1	1999Y-144-PG	460	18-Apr-1999	1.0957	0.0067	89.2
1999Y-2	1999Y-144-PG	430	18-Apr-1999	1.0872	0.0067	80.8
1999Y-3	1999Y-146-PG	400	17-Apr-1999	1.1073	0.0066	100.8
1999Y-4	1999Y-146-PG	400	17-Apr-1999	1.0886	0.0068	82.2
2003B-3	1999B-144-PG	450	24-Oct-2003	1.0666	0.0069	59.8
2003B-4	1999B-144-PG	430	11-Oct-2003	1.0695	0.0063	62.6
2003B-5	1999B-144-PG	400	20-Oct-2003	1.0617	0.0076	54.8
2003S-1	2003S-148-PG	310	22-Oct-2003	1.0777	0.0064	70.7
2003Y-1	2003Y-148-PG	470	2-Oct-2003	1.0776	0.0077	70.7
2003Y-2	2003Y-147-PG	440	20-Oct-2003	1.0822	0.0076	75.2
2003Y-3	2003Y-148-PG	420	11-Oct-2003	1.0812	0.0066	74.2
2003Y-4	2003Y-149-PG	360	15-Oct-2003	1.0813	0.0064	74.3
2003Y-5	2003Y-148-PG	350	24-Oct-2003	1.0712	0.0078	64.3
2004B-1	2004B-148-PG	470	28-Aug-2004	1.0670	0.0079	60.0
2004B-2	2004B-146-PG	450	14-Sep-2004	1.0794	0.0097	72.3
2004B-3	2004B-145-PG	280	18-Sep-2004	1.0758	0.0076	68.7
2004S-1	2004S-145-PG	300	18-Sep-2004	1.0744	0.0071	67.4
2004Y-1	2004Y-148-PG	400	26-Aug-2004	1.0685	0.0065	61.5
2004Y-2	2004Y-146-PG	300	14-Sep-2004	1.0786	0.0079	71.5
2004Y-3	2004Y-145-PG	290	18-Sep-2004	1.0771	0.0069	70.0
2004Y-4	2004Y-145-PG	280	18-Sep-2004	1.0803	0.0068	73.2
2005B-1	2005B-149-PG	470	1-Sep-2005	1.0657	0.0069	58.6
2005B-2	2005B-150-PG	460	28-Aug-2005	1.0789	0.0069	71.7
2005B-3	2005B-147-PG	440	5-Jun-2005	1.0725	0.0063	65.4
2005B-4	2005B-156-PG	330	15-Mar-2005	1.0761	0.0079	69.0
2005B-5	2005B-155-PG	290	4-Mar-2005	1.0789	0.0064	71.8

2005S-1	2005S-147-PG	300	1-Jun-2005	1.0639	0.0068	56.9
2005Y-1	2005Y-150-PG	420	27-Aug-2005	1.0793	0.0075	72.1
2005Y-2	2005Y-150-PG	380	30-Aug-2005	1.0820	0.0069	74.8
2005Y-3	2005Y-155-PG	290	2-Mar-2005	1.0855	0.0082	78.3
2005Y-3	2005Y-155-PG	300	11-Mar-2005	1.0768	0.0068	69.7
2005Y-4	2005Y-147-PG	290	1-Jun-2005	1.0696	0.0066	62.5
2006B-1	2006B-142-PG	430	31-Oct-2006	1.0761	0.0075	68.8
2006B-2	2006B-148-PG	340	12-May-2006	1.0716	0.0065	64.3
2006B-3	2006B-148-PG	300	11-May-2006	1.0898	0.0077	82.5
2006B-4	2006B-146-PG	290	4-Oct-2006	1.0810	0.0068	73.7
2006B-5	2006B-146-PG	280	29-Oct-2006	1.0703	0.0065	63.0
2006S-1	2006S-147-PG	300	13-May-2006	1.0703	0.0063	63.1
2006Y-1	2006Y-149-PG	340	26-Oct-2006	1.0755	0.0067	68.2
2006Y-2	2006Y-146-PG	320	29-Oct-2006	1.0839	0.0079	76.5
2006Y-3	2006Y-142-PG	310	31-Oct-2006	1.0595	0.0078	52.3
2006Y-4	2006Y-145-PG	290	17-Oct-2006	1.0709	0.0072	63.6
2006Y-5	2006Y-145-PG	290	17-Oct-2006	1.0548	0.0063	47.6
2006Y-6	2006Y-148-PG	260	11-May-2006	1.0858	0.0074	78.4
2006Y-7	2006Y-148-PG	250	11-May-2006	1.0681	0.0063	60.8
2009B-1	2009B-161-I2	470	30-Oct-2009	1.0680	0.0062	60.3
2009B-2	2009B-173-TV	400	26-Mar-2009	1.0511	0.0061	43.7
2009B-3	2009B-176-TV	330	17-Jun-2009	1.0479	0.0061	40.4
2009B-4	2009B-176-TV	320	17-Jun-2009	1.0527	0.0061	45.1
2009Y-1	2009Y-174-TV	380	27-Mar-2009	1.0489	0.0077	41.4
2009Y-2	2009Y-165-NR	380	9-Oct-2009	1.0736	0.0076	65.9
2009Y-3	2009Y-165-NR	320	12-Oct-2009	1.0682	0.0078	60.6
2009Y-4	2009Y-172-I2	300	15-Oct-2009	1.0781	0.0076	70.4
2010B-1	2010B-187-TO	490	14-Jul-2010	1.0522	0.0076	44.5
2010B-2	2010B-189-PX	480	21-Nov-2010	1.0498	0.0069	42.1
2011Y-1	2011Y-149-PG	390	11-May-2011	1.0600	0.0069	52.2
2011Y-2	2011Y-148-PG	390	14-May-2011	1.0697	0.0082	61.8
2011Y-3	2011Y-149-PG	380	11-May-2011	1.0652	0.0085	57.4
2011Y-4	2011Y-148-PG	370	14-May-2011	1.0614	0.0065	53.6
2013B-1	2013B-154-PG	460	30-Aug-2013	1.0464	0.0078	38.5
2013B-2a	2013B-159-PG	440	7-Oct-2013	1.0489	0.0079	40.9
2013B-2b	2013B-179-FJ	430	6-Jun-2013	1.0587	0.0075	50.6
2013B-3a	2013B-189-PX	420	22-Nov-2013	1.0673	0.0083	59.1
2013B-3b	2013B-179-FJ	430	28-May-2013	1.0581	0.0076	50.0
2013B-4	2013B-161-PG	410	28-Apr-2013	1.0616	0.0077	53.5
2013B-5	2013B-145-PG	360	14-May-2013	1.0417	0.0075	33.8
2013S-1	2013S-145-PG	290	14-May-2013	1.0459	0.0077	37.9
2013S-2	2013S-181-FJ	430	15-May-2013	1.0437	0.0074	35.8
2013S-3	2013S-200-CK	460	15-Apr-2013	1.0536	0.0075	45.6
2013S-4	2013S-181-CK	500	15-Dec-2013	1.0525	0.0074	44.4
2013Y-1	2013Y-200-CK	500	16-Apr-2013	1.0481	0.0077	40.1
2013Y-2	2013Y-189-PX	450	22-Nov-2013	1.0464	0.0081	38.3
2013Y-3	2013Y-159-PG	400	7-Oct-2013	1.0662	0.0078	58.1
2013Y-4	2013Y-149-PG	330	23-Apr-2013	1.0523	0.0075	44.3
2013Y-5	2013Y-145-PG	300	13-May-2013	1.0471	0.0075	39.2
2013Y-6	2013Y-200-CK	490	5-Apr-2013	1.0500	0.0075	42.1
2014B-1	2014B-169-GL	500	9-Mar-2014	1.0699	0.0080	61.6
2014B-2	2014B-188-TK	460	21-Aug-2014	1.0392	0.0076	31.1

2014B-3	2014B-160-PG	420	4-Aug-2014	1.0463	0.0075	38.2
2014Y-1	2014Y-157-SB	480	27-Aug-2014	1.0386	0.0076	30.5
2014Y-2	2014Y-160-PG	480	30-Jul-2014	1.0585	0.0076	50.3
2014Y-3	2014Y-160-FM	450	25-Aug-2014	1.0476	0.0075	39.5
2014Y-4	2014Y-166-NR	450	17-May-2014	1.0438	0.0076	35.8
2015B-1	2015B-143-PG	480	19-Nov-2015	1.0630	0.0083	54.6
2015B-2	2015B-219-I6	350	19-Oct-2015	1.0658	0.0084	57.4
2015S-1	2015S-147-PG	340	16-Nov-2015	1.0327	0.0074	24.6
2015S-2	2015S-188-WS	470	5-Feb-2015	1.0413	0.0075	33.1
2015S-3	2015S-188-WS	500	5-Feb-2015	1.0391	0.0076	31.0
2015S-4	2015S-195-CK	480	16-Feb-2015	1.0476	0.0075	39.4
2015S-5	2015S-195-CK	450	16-Feb-2015	1.0348	0.0075	26.7
2016B-1	2016B-159-PG	480	7-Nov-2016	1.0538	0.0075	45.3
2016S-1	2015S-178-FJ	500	18-Mar-2016	1.0401	0.0076	31.8
2017B-1	2017B-190-PX	480	9-Oct-2017	1.0308	0.0074	22.4
2017B-2	2017B-203-LN	410	16-May-2017	1.0424	0.0076	33.9
2017B-3	2017B-192-PX	410	1-Oct-2017	1.0335	0.0074	25.1
2017B-4	2017B-201-LN	320	29-May-2017	1.0490	0.0076	40.6
2017S-1	2017S-150-PG	310	2-Oct-2017	1.0293	0.0076	20.9
2017Y-1	2017Y-160-PG	440	6-Jan-2017	1.0476	0.0083	39.1
2017Y-2	2017Y-192-PX	430	1-Oct-2017	1.0390	0.0066	30.6
2017Y-3	2017Y-157-SB	420	19-Oct-2017	1.0608	0.0084	52.2
2017Y-4	2017Y-150-PG	380	24-Sep-2017	1.0452	0.0076	36.7
2017Y-5	2017Y-233-I6	370	9-Jun-2017	1.0312	0.0074	22.9
2017Y-5	2017Y-204-LN	300	18-May-2017	1.0281	0.0074	19.8
2018B-1	2018B-179-TV	500	9-Mar-2018	1.0321	0.0077	23.6
2018B-2	2018B-165-NR	460	22-Jul-2018	1.0306	0.0074	22.1
2018B-3	2018B-173-TV	330	30-Jul-2018	1.0515	0.0075	42.9
2018B-4	2019B-157-PG	490	18-Sep-2019	1.0387	0.0075	30.0
2018B-5	2019B-147-PG	390	29-Jul-2019	1.0329	0.0074	24.3
2019-S1	2019S-148-PG	400	28-Jul-2019	1.0355	0.0074	26.9
2019Y-1	2019Y-171-GL	420	19-Jun-2019	1.0493	0.0076	40.5
2019Y-2	2019Y-148-PG	410	28-Jul-2019	1.0391	0.0085	30.5
2019Y-3	2019Y-157-SB	390	21-Apr-2019	1.0363	0.0073	27.6
2019Y-4	2019Y-176-GL	390	1-Jul-2019	1.0573	0.0073	48.5
2019Y-5	2019Y-140-I2	330	2-Aug-2019	1.0372	0.0080	28.5
2019Y-6	2019Y-157-SB	320	21-Apr-2019	1.0409	0.0075	32.3
2019Y-7	2019Y-177-GL	320	18-Oct-2019	1.0279	0.0073	19.3

Table 2. Fish and otolith information with corresponding ^{14}C data for BET yoy that were measured prior to this study (K. Okamoto and K. Satoh, unpublished data). The collection date and location for some fish (**) was not precisely known and may have been 4 to 28 days later than the date listed and ±0.5–9.5° latitude and ±0.5–8.5° longitude relative to the location plotted (Figure 3) — these potential offsets were insignificant relative to the date-of-formation used in ^{14}C calculations and in terms of location variability as a regional ^{14}C reference.

Lab number	SL (mm)	SFL (mm)*	Capture date	$F^{14}C$	$\Delta^{14}C$ (‰)
2010B-25JP	268	276	26-Dec-2010	1.0567	49.1
2010B-05JP	295	304	19-Dec-2010	1.0650	57.3
2012B-01JP	413	425	2-Sep-2012	1.0607	52.7
2012B-02JP	428	440	2-Sep-2012	1.0608	52.9
2012B-03JP**	428	440	28-Oct-2012	1.0644	56.4
2012B-04JP**	433	445	28-Oct-2012	1.0673	59.3
2013B-10JP**	390	401	23-Dec-2013	1.0558	47.8
2013B-09JP	403	415	7-Oct-2013	1.0603	52.2
2013B-08JP	355	366	7-Oct-2013	1.0621	54.0
2013B-27JP**	307	316	11-Oct-2013	1.0554	47.4
2013B-26JP**	261	269	4-Feb-2013	1.0554	47.4
2013B-06JP**	405	417	16-Oct-2013	1.0585	50.5
2013B-07JP**	415	427	16-Oct-2013	1.0589	50.9
2013B-29JP	402	414	28-Oct-2013	1.0465	38.5
2013B-28JP	395	407	28-Oct-2013	1.0553	47.2
2014B-11JP	450	463	23-Mar-2014	1.0614	53.3
2014B-12JP**	351	361	21-Sep-2014	1.0555	47.4
2015B-13JP**	397	409	14-Feb-2015	1.0520	43.7
2017B-16JP**	373	384	7-Jun-2017	1.0409	32.5
2017B-15JP**	364	375	7-Jun-2017	1.0426	34.2
2017B-19JP	325	335	2-Nov-2017	1.0474	38.9
2017B-14JP**	388	399	7-Apr-2017	1.0461	37.7
2017B-18JP**	389	400	9-Oct-2017	1.0438	35.3
2017B-17JP**	393	405	9-Oct-2017	1.0492	40.8
2018B-20JP**	415	427	12-May-2018	1.0494	40.8
2018B-23JP**	402	414	12-May-2018	1.0517	43.1
2018B-24JP**	331	341	22-Jun-2018	1.0482	39.6
2018B-21JP**	341	351	13-Jun-2018	1.0351	26.6
2018B-22JP**	398	410	13-Jun-2018	1.0562	47.5

* Straight fork length (SFL) calculated as ~3% greater that the measured standard length (SL).

Table 3. Fish, otolith, and age estimate information with corresponding ^{14}C data for the 77 older aged YFT specimens used in this study. Specific capture date was used to calculate the year-of-formation by subtracting age (years) and adding 0.5 years to account for core formation period. Fish length is provided as straight fork length (SFL) in mm, whole otolith mass in grams for intact otoliths only. Radiocarbon measurements are listed as $F^{14}C$ with instrument measurement error and as formation-date-corrected $\Delta^{14}C$ in per mille (Reimer et al., 2004). Outliers are denoted in bold type.

Lab number	Capture	SFL (mm)	Mass (g)	Age (yr)	YoF	$F^{14}C$	Err (abs)	$\Delta^{14}C$ (‰)
2013Y-129	19-Dec-13	129	0.0605	4.1	2010.40	1.0631	0.0072	55.4
2013Y-154	25-Dec-13	154	NA	10.4	2004.13	1.0746	0.0063	67.6
2013Y-156	13-Nov-13	156	0.1095	13.8	2000.54	1.0838	0.0072	77.2
2014Y-092	8-Aug-14	92	0.0327	2.0	2013.11	1.0657	0.0076	57.5
2014Y-095	13-May-14	95	0.0276	1.9	2012.92	1.0560	0.0074	48.0
2014Y-096	23-Sep-14	96	0.0356	2.3	2012.92	1.0568	0.0071	48.7
2014Y-110	22-May-14	110	0.0523	3.4	2011.44	1.0485	0.0072	40.7
2014Y-116	29-Mar-14	116	0.0544	3.3	2011.41	1.0573	0.0079	49.5
2014Y-120	13-Nov-14	120	0.0409	2.9	2012.45	1.0554	0.0068	47.5
2014Y-123	21-May-14	123	0.0560	3.1	2011.79	1.0570	0.0072	49.1
2014Y-126A	**16-Aug-14**	**126**	**0.0489**	**3.3**	**2011.83**	**1.0834**	**0.0072**	**75.3**
2014Y-126B	18-May-14	126	0.0488	3.1	2011.76	1.0629	0.0073	55.0
2014Y-128	27-Jun-14	128	NA	4.3	2010.65	1.0590	0.0069	51.3
2014Y-130	31-Jul-14	130	0.0691	4.3	2010.74	1.0700	0.0071	62.1
2014Y-131	26-Jan-14	131	0.0731	7.6	2006.97	1.0863	0.0073	78.8
2014Y-132A	29-Sep-14	132	0.0822	8.8	2006.42	1.0597	0.0070	52.5
2014Y-132B	14-Oct-14	132	NA	6.6	2008.73	1.0585	0.0069	51.0
2014Y-135A	5-Nov-14	135	0.1159	8.5	2006.83	1.0558	0.0065	48.6
2014Y-135B	27-Jun-14	135	0.0721	6.2	2008.79	1.0834	0.0072	75.7
2014Y-137	30-Sep-14	137	0.0712	6.6	2008.67	1.0572	0.0069	49.7
2014Y-140	4-Apr-14	140	0.0790	9.4	2005.40	1.0625	0.0065	55.4
2014Y-141	27-Jun-14	141	0.0720	5.3	2009.69	1.0708	0.0065	63.1
2014Y-145	**13-Sep-14**	**145**	**0.1056**	**11.2**	**2003.50**	**1.0548**	**0.0065**	**48.0**
2014Y-146	13-Sep-14	146	NA	8.1	2006.97	1.0691	0.0066	61.8
2014Y-150	22-Aug-14	150	0.1034	11.5	2003.69	1.0843	0.0071	77.3
2014Y-151	6-Feb-14	151	NA	8.0	2006.62	1.0704	0.0063	63.1
2014Y-153	22-Aug-14	153	0.0885	10.8	2004.37	1.0793	0.0072	72.2
2015Y-077	26-Apr-15	77	0.0263	1.7	2014.14	1.0516	0.0068	43.5
2015Y-079	11-Apr-15	79	0.0227	1.5	2014.32	1.0574	0.0068	49.2
2015Y-082	21-Aug-15	82	0.0249	1.3	2014.80	1.0532	0.0068	45.0
2015Y-089	2-Jul-15	89	0.0308	1.6	2014.40	1.0454	0.0068	37.3
2015Y-120	29-Oct-15	120	0.0457	3.6	2012.75	1.0389	0.0069	31.0
2015Y-129	30-Aug-15	129	NA	5.4	2010.78	1.0688	0.0070	61.0
2015Y-131	15-Aug-15	131	0.0572	4.8	2011.37	1.0530	0.0069	45.2
2015Y-132	30-Jul-15	132	NA	7.6	2008.46	1.0514	0.0069	44.0
2015Y-140	4-Oct-15	140	0.0797	6.4	2009.90	1.0668	0.0064	59.1
2015Y-144	7-Dec-15	144	0.0696	5.5	2010.95	1.0561	0.0065	48.4
2015Y-150	14-Jan-15	150	0.1188	7.2	2008.36	1.0745	0.0072	66.9
2015Y-152	8-Jan-15	152	NA	8.8	2006.76	1.0661	0.0069	58.8
2015Y-156	7-Mar-15	156	0.1199	9.4	2006.33	1.0691	0.0065	61.8
2015Y-164	24-Jan-15	164	0.0911	6.5	2009.09	1.0672	0.0063	59.6
2016Y-074	5-Jun-16	74	0.0226	1.5	2015.43	1.0467	0.0068	38.5
2016Y-128	5-Apr-16	128	0.0609	4.9	2011.91	1.0590	0.0070	51.1
2016Y-146	8-Mar-16	146	0.0904	7.4	2009.28	1.0668	0.0064	59.2

2016Y-172	4-Mar-16	172	0.1322	10.9	2005.81	1.0674	0.0064	60.2
2017Y-079	**1-Nov-17**	**79**	**0.0215**	**1.2**	**2017.15**	**1.0744**	**0.0073**	**65.7**
2017Y-101A	23-Feb-17	101	0.0368	2.5	2015.15	1.0559	0.0071	47.6
2017Y-101B	21-Jan-17	101	0.0319	2.0	2015.56	1.0623	0.0073	53.9
2017Y-103	16-Apr-17	103	0.0406	2.5	2015.25	1.0562	0.0072	47.9
2017Y-109	27-May-17	109	0.0402	2.3	2015.60	1.0577	0.0072	49.4
2017Y-112	28-Feb-17	112	0.0410	3.0	2014.68	1.0516	0.0072	43.4
2017Y-117	10-Oct-17	117	0.0505	2.9	2015.35	1.0520	0.0070	43.8
2017Y-133	18-Sep-17	133	NA	11.7	2006.55	NM	--	--
2017Y-140	21-Aug-17	140	0.0816	6.5	2011.63	1.0521	0.0068	44.3
2017Y-142	29-May-17	142	0.0634	5.3	2012.64	1.0530	0.0063	45.0
2017Y-146A	16-Dec-17	146	0.1163	9.8	2008.66	1.0585	0.0064	51.0
2017Y-146B	3-Jul-17	146	0.0826	7.2	2010.82	1.0694	0.0073	61.6
2017Y-148	7-Dec-17	148	0.1406	7.7	2010.71	1.0564	0.0066	48.6
2017Y-151A	9-Sep-17	151	NA	10.2	2008.00	1.0693	0.0073	61.9
2017Y-151B	13-Sep-17	151	0.1143	8.5	2009.70	1.0569	0.0072	49.3
2017Y-152	16-Dec-17	152	0.1214	8.8	2009.66	1.0589	0.0072	51.3
2017Y-153	28-May-17	153	0.1026	12.2	2005.68	1.0658	0.0074	58.6
2017Y-155A	2-Sep-17	155	0.1230	12.9	2005.24	1.0785	0.0063	71.3
2017Y-155B	2-Sep-17	155	NA	8.7	2009.46	1.0724	0.0073	64.8
2017Y-156A	21-Aug-17	156	NA	10.2	2007.98	1.0753	0.0065	67.8
2017Y-156B	9-Dec-17	156	0.0968	7.6	2010.88	1.0780	0.0063	70.1
2017Y-157	22-Aug-17	157	NA	11.3	2006.86	1.0708	0.0062	63.5
2018Y-125	21-Oct-18	125	0.0561	5.0	2014.26	1.0436	0.0072	35.5
2018Y-136	23-Jul-18	136	0.0621	4.0	2015.04	1.0647	0.0069	56.4
2018Y-137	3-Apr-18	137	0.0702	4.1	2014.65	1.0625	0.0072	54.2
2018Y-147	22-Oct-18	147	0.1081	8.3	2010.96	1.0604	0.0064	52.6
2018Y-148	5-Dec-18	148	NA	10.4	2009.06	1.0771	0.0080	69.5
2018Y-150A	**5-Dec-18**	**150**	**NA**	**9.7**	**2009.77**	**1.0904**	**0.0082**	**82.5**
2018Y-150B	12-Oct-18	150	0.0951	8.8	2010.48	1.0767	0.0074	68.8
2018Y-155	4-Apr-18	155	0.0947	8.2	2010.59	1.0507	0.0067	43.0
2018Y-160	26-Jan-18	160	0.1118	9.0	2009.61	1.0509	0.0078	43.4
2019Y-147	11-Mar-19	147	0.0778	7.4	2012.31	1.0528	0.0069	44.9

NM - This sample was lost during the sampling process and was not measured.

Table 4. Fish, otolith, and age estimate information with corresponding ^{14}C data for the 65 older aged BET specimens used in this study. Specific capture date was used to calculate the year-of-formation by subtracting age (years) and adding 0.5 years to account for core formation period. Fish length is provided as straight fork length (SFL) in mm, whole otolith mass in grams for intact otoliths only. Radiocarbon measurements are listed as $F^{14}C$ with instrument measurement error and as formation-date-corrected $\Delta^{14}C$ in per mille (Reimer et al., 2004).

Lab number	Capture	SFL (mm)	Mass (g)	Age (yr)	YoF	$F^{14}C$	Err (abs)	$\Delta^{14}C$ (‰)
2014B-066	13-Aug-14	66	0.0203	1.3	2013.583	1.0356	0.0071	27.7
2014B-077	29-Dec-14	77	0.0233	1.2	2014.090	1.0429	0.0071	34.8
2014B-094	18-Jun-14	94	0.0399	2.7	2012.275	1.0444	0.0071	36.6
2014B-095	15-Jul-14	95	0.0339	2.1	2012.970	1.0443	0.0072	36.4
2014B-104	23-Sep-14	104	0.0547	2.8	2012.457	1.0596	0.0072	51.7
2014B-105	28-Sep-14	105	0.0493	2.4	2012.884	1.0502	0.0071	42.2
2014B-111	04-Nov-14	111	0.0546	3.5	2011.869	1.0470	0.0071	39.2
2014B-116	27-Jun-14	116	NA	4.0	2010.994	1.0660	0.0076	58.2
2014B-126	13-Mar-14	126	0.0668	5.4	2009.328	1.0437	0.0072	36.2
2014B-128	27-May-14	128	0.0745	5.4	2009.498	1.0539	0.0072	46.3
2014B-132	03-May-14	132	NA	9.0	2005.832	1.0806	0.0088	73.4
2014B-135A	26-May-14	135	NA	5.5	2009.417	1.0621	0.0075	54.5
2014B-135B	22-Oct-14	135	0.0652	5.4	2009.889	1.0682	0.0073	60.5
2014B-136A	15-Mar-14	136	0.0704	7.9	2006.772	1.0548	0.0072	47.6
2014B-136B	07-May-14	136	0.1096	7.5	2007.321	1.0523	0.0071	45.0
2014B-136C	07-Oct-14	136	0.0736	5.3	2009.991	1.0714	0.0073	63.6
2014B-138	22-Aug-14	138	NA	7.0	2008.123	1.0535	0.0075	46.1
2014B-139A	02-Dec-14	139	0.0844	9.8	2005.579	1.0700	0.0068	62.9
2014B-139B	14-Oct-14	139	0.0739	7.0	2008.286	1.0611	0.0067	53.6
2014B-140A	03-Dec-14	140	NA	7.7	2007.716	1.0594	0.0065	52.0
2014B-140B	08-Jul-14	140	0.0867	6.4	2008.575	1.0569	0.0063	49.5
2014B-143	02-Dec-14	143	0.0734	6.5	2008.873	1.0653	0.0070	57.7
2014B-145A	25-Nov-14	145	0.1235	9.7	2005.708	1.0780	0.0064	70.8
2014B-145B	27-Nov-14	145	NA	9.2	2006.221	1.0734	0.0065	66.1
2014B-145C	24-May-14	145	0.0918	7.5	2007.441	1.0691	0.0064	61.7
2014B-147	26-May-14	147	0.0946	6.3	2008.571	1.0691	0.0064	61.6
2014B-148	17-Jun-14	148	0.1070	8.3	2006.638	1.0595	0.0063	52.3
2014B-154	17-Aug-14	154	0.1111	8.7	2006.390	1.0597	0.0064	52.5
2014B-157	17-Jul-14	157	0.0849	7.8	2007.255	1.0724	0.0065	65.0
2015B-063	17-Oct-15	63	0.0195	1.2	2015.064	1.0456	0.0096	37.4
2015B-081	07-Jan-15	81	0.0350	1.4	2014.098	1.0512	0.0075	43.1
2015B-084	11-Jun-15	84	0.0284	1.7	2014.247	1.0561	0.0072	47.9
2015B-086	17-Apr-15	86	0.0307	1.5	2014.255	1.0474	0.0079	39.3
2015B-101A	30-Dec-15	101	0.0366	2.4	2014.064	NM	--	--
2015B-101B	31-May-15	101	0.0439	2.0	2013.894	1.0504	0.0074	42.4
2015B-113	07-Apr-15	113	0.0452	3.2	2012.556	1.0605	0.0075	52.5
2015B-116	16-May-15	116	0.0635	3.7	2012.204	1.0523	0.0067	44.4
2015B-120	08-Feb-15	120	0.0630	3.7	2011.933	1.0539	0.0075	46.0
2015B-122A	02-Jun-15	122	0.0638	4.3	2011.574	1.0608	0.0076	52.9
2015B-122B	07-Jan-15	122	0.0623	4.2	2011.294	1.0566	0.0070	48.8
2015B-122C	18-Dec-15	122	0.0551	3.8	2012.706	1.0618	0.0075	53.7
2015B-122D	01-Jan-15	122	0.0564	3.2	2012.297	1.0541	0.0074	46.2
2015B-123A	20-May-15	123	0.0575	4.6	2011.287	1.0648	0.0068	56.9
2015B-123B	15-Nov-15	123	0.0664	4.3	2012.055	1.0568	0.0074	48.9

2015B-126	09-May-15	126	0.0657	5.6	2010.281	1.0469	0.0068	39.3
2015B-127	08-May-15	127	0.0614	4.7	2011.188	1.0523	0.0074	44.6
2015B-129	29-Jan-15	129	0.0669	4.8	2010.734	1.0667	0.0075	58.9
2015B-130	09-May-15	130	0.0702	5.5	2010.328	1.0606	0.0068	52.8
2015B-132	09-May-15	132	0.0592	5.3	2010.527	1.0729	0.0075	65.1
2015B-133A	25-Jan-15	133	0.0826	7.6	2007.927	1.0678	0.0067	60.3
2015B-133B	09-May-15	133	0.0865	6.5	2009.355	1.0638	0.0068	56.2
2015B-133C	20-May-15	133	0.0646	4.5	2011.374	1.0596	0.0067	51.8
2015B-136	01-Feb-15	136	0.1015	7.4	2008.225	1.0607	0.0070	53.2
2015B-137	05-Jun-15	137	0.0823	8.6	2007.312	1.0851	0.0073	77.6
2015B-139	13-Mar-15	139	0.0793	6.2	2009.478	1.0624	0.0070	54.8
2015B-140A	01-Feb-15	140	0.0811	7.9	2007.664	1.0644	0.0074	57.0
2015B-140B	22-Sep-15	140	0.0773	5.7	2010.512	1.0703	0.0076	62.5
2015B-141	05-May-15	141	0.1191	13.0	2002.824	1.0836	0.0066	76.7
2015B-142	02-Apr-15	142	0.1009	8.3	2007.403	1.0661	0.0068	58.8
2015B-143	03-Apr-15	143	0.1083	8.6	2007.152	1.0714	0.0064	64.0
2015B-145A	01-Feb-15	145	0.0951	8.3	2007.303	1.0628	0.0073	55.5
2015B-145B	09-May-15	145	0.0861	6.9	2008.997	1.0619	0.0073	54.4
2015B-146	23-Jun-15	146	NA	7.7	2008.238	1.0645	0.0064	57.0
2015B-151	18-Jun-15	151	0.0951	6.9	2009.035	1.0670	0.0065	59.4
2015B-157	19-Mar-15	157	0.1003	6.6	2009.158	1.0659	0.0065	58.3

NM - This sample was lost during the sampling process and was not measured.

Table 5. Juvenile-to-adult ^{14}C uptake for YFT. All NC collections. Rise may be related to GBR record (Wu et al. 2021). YoF = year of formation calculated as an adjusted date for central time of estimated formation period of the extracted sample: core adjusted by 0.5 years (1-year period) and tip adjusted by 1.5 years (3-year period). Span is the number of years between the central dates of formation for each fish. Outliers are highlighted in bold type.

Lab number	Capture date	SFL (mm)	Otolith mass (mg)	Age (years)	$F^{14}C$	YoF (core-tip)	Span (years)
2015Y-156	7-Mar-15	156	0.1199	9.4	1.0691	2006.33	
2015Y-156T	8-Mar-15	156	0.1199	9.4	1.0697	2013.68	7.36
2017Y-146A	16-Dec-17	146	0.1163	9.8	1.0585	2008.66	
2017Y-146AT	16-Dec-17	146	0.1163	9.8	1.0573	2016.46	7.80
2017Y-151A	9-Sep-17	151	NA	10.2	1.0693	2008.00	
2017Y-151AT	10-Sep-17	151	NA	10.2	1.0584	2016.19	8.19
2017Y-151B	13-Sep-17	151	0.1143	8.5	1.0569	2009.70	
2017Y-151BT	13-Sep-17	151	0.1143	8.5	1.0595	2016.20	6.51
2017Y-152	16-Dec-17	152	0.1214	8.8	1.0589	2009.66	
2017Y-152T	**16-Dec-17**	**152**	**0.1214**	**8.8**	**1.0715**	**2016.46**	6.80
2017Y-153	28-May-17	153	0.1026	12.2	1.0658	2005.68	
2017Y-153T	28-May-17	153	0.1026	12.2	1.0557	2015.91	10.23
2017Y-155A	2-Sep-17	155	0.1230	12.9	1.0785	2005.24	
2017Y-155AT	2-Sep-17	155	0.1230	12.9	1.0616	2016.17	10.93
2017Y-157	22-Aug-17	157	NA	11.3	1.0708	2006.86	
2017Y-157T	**22-Aug-17**	**157**	**NA**	**11.3**	**1.0719**	**2016.14**	9.28
2018Y-150A	5-Dec-18	150	NA	9.7	1.0904*	--	
2018Y-150AT	5-Dec-18	150	NA	9.7	NM**	--	

* Otolith sample value was elevated and deemed an outlier for unknown reasons.

** Not measured due to no gas generated from the sample for unknown reasons.

Table 6. Juvenile-to-adult ^{14}C uptake for BET. Unlike YFT, the collection locations are broadly distributed. The stronger concordance of the data from the most recently formed part of the otolith may be due to the known vertical migration behavior in the mixed layer. YoF = year-of-formation calculated as an adjusted date for central time of estimated formation period of the extracted sample: core adjusted by 0.5 years (1-year period) and tip adjusted by 1.5 years (3-year period). Span is the number of years between the central dates of formation for each fish.

Lab number	Capture date	SFL (mm)	Otolith mass (mg)	Age (years)	$F^{14}C$	YoF (core-tip)	Span (years)
2014B-136B	7-May-14	136	0.1096	7.5	1.0523	2007.32	
2014B-136BT	7-May-14	136	0.1096	7.5	1.0543	2012.85	5.53
2014B-145A	25-Nov-14	145	0.1235	9.7	1.0780	2005.71	
2014B-145AT	25-Nov-14	145	0.1235	9.7	1.0535	2013.40	7.69
2014B-145B	27-Nov-14	145	NA	9.2	1.0734	2006.22	
2014B-145BT	27-Nov-14	145	NA	9.2	1.0495	2013.41	7.19
2014B-148	17-Jun-14	148	0.1070	8.3	1.0595	2006.64	
2014B-148T	17-Jun-14	148	0.1070	8.3	1.0472	2012.96	6.32
2014B-154	17-Aug-14	154	0.1111	8.7	1.0597	2006.39	
2014B-154T	17-Aug-14	154	0.1111	8.7	1.0587	2013.13	6.74
2014B-157	17-Jul-14	157	0.0849	7.8	1.0724	2007.25	
2014B-157T	17-Jul-14	157	0.0849	7.8	1.0454	2013.04	5.79
2015B-136	1-Feb-15	136	0.1015	7.4	1.0607	2008.23	
2015B-136T	1-Feb-15	136	0.1015	7.4	1.0485	2013.59	5.36
2015B-143	3-Apr-15	143	0.1083	8.6	1.0714	2007.15	
2015B-143T	3-Apr-15	143	0.1083	8.6	1.0545	2013.76	6.60
2015B-145A	1-Feb-15	145	0.0951	8.3	1.0628	2007.30	
2015B-145AT	1-Feb-15	145	0.0951	8.3	1.0453	2013.59	6.29
2015B-151	18-Jun-15	151	0.0951	6.9	1.0670	2009.03	
2015B-151T	18-Jun-15	151	0.0951	6.9	1.0458	2013.96	4.93
2015B-157	19-Mar-15	157	0.1003	6.6	1.0659	2009.16	
2015B-157T	19-Mar-15	157	0.1003	6.6	1.0308*	2013.71	4.56

* Otolith sample value was depleted for the edge measurement possibly due to greater influence of deeper, ^{14}C-depleted waters for this individual.